
Equilibrated gas and carbonate standard-derived paired clumped isotope (Δ_{47} and Δ_{48}) values on the absolute reference frame

Rapid Communications in Mass Spectrometry

Jamie K. Lucarelli[1], Hannah M. Carroll[1], Ben M. Elliott[1], Robert A. Eagle[1], Aradhna Tripati[1]

[1]Department of Earth, Planetary, and Space Sciences, Department of Atmospheric and Oceanic Sciences, Institute of the Environment and Sustainability, Center for Diverse Leadership in Science, UCLA, Los Angeles, CA 90095 USA.

Correspondence to: jklucarelli@gmail.com and atripati@g.ucla.edu

Running Head: Robust Methods for Paired Carbonate Clumped Isotope Analysis (Δ_{47} and Δ_{48}) via IRMS

Equilibrated gas and carbonate standard-derived paired clumped isotope (Δ_{47} and Δ_{48}) values on the absolute reference frame

Journal:	*Rapid Communications in Mass Spectrometry*
Manuscript ID	Draft
Wiley - Manuscript type:	Research Article
Date Submitted by the Author:	n/a
Complete List of Authors:	Lucarelli, Jamie; University of California Los Angeles, Earth, Planetary & Space Sciences Carroll, Hannah; University of California Los Angeles, Department of Earth, Planetary, and Space Sciences, Department of Atmospheric and Oceanic Sciences, Institute of the Environment and Sustainability, Center for Diverse Leadership in Science Elliott, Ben; University of California Los Angeles, Earth, Planetary & Space Sciences Eagle, Robert; University of California Los Angeles Tripati, Aradhna; University of California Los Angeles, Department of Earth, Planetary, and Space Sciences; Department of Atmospheric and Oceanic Sciences; Institute for the Environment and Sustainability; California Nanosystems Institute
Keywords:	clumped isotopes, Δ47, Δ48, paleoclimate, Devils Hole
Abstract:	Rationale: Carbonate clumped isotope geochemistry has primarily focused on mass spectrometric determination of mass-47 CO_2 for geothermometry, but theoretical calculations indicate paired analysis of the mass-47 (^{13}C-^{18}O-^{16}O) and mass-48 (^{12}C-^{18}O-^{18}O) isotopologues (denoted with Δ_{47} and Δ_{48} notation) can be used to study non-equilibrium isotope fractionations and refine temperature estimates. We are one of two labs currently utilizing paired Δ_{47} and Δ_{48} measurements to study equilibrium and kinetic isotope effects in carbonates. Additional work is needed on different instruments to define standard Δ_{48} values against equilibrated gases and evaluate Δ_{48} values using carbonate transfer functions. Methods: We determined Δ_{47} and Δ_{48} of standards using isotope ratio mass spectrometry during the time interval of 2015-2021 on a Thermo Fischer MAT 253 mass spectrometer with a common acid bath digestion system and two Nu Instruments Perspective mass spectrometers with common acid bath and individual reaction vessel digestion systems. A total of 5,581 Δ_{47} and 4,212 Δ_{48} measurements of carbonates, and 183 Δ_{47} and 195 Δ_{48} measurements of gas standards are used from robust correction intervals over multiple years. We report statistical methods for data screening and quality assurance.

	Results: Equilibrated gas-based standard values support the accuracy of the recently proposed $\Delta_{47\ I\text{-}CDES}$ reference frame and provide robust constraints on Δ_{48} values for carbonate standards. We provide further constraints on the equilibrium Δ_{47} vs Δ_{48} relationship and report values of Devils Hole cave calcite. We demonstrate regression-based acid digestion fractionation factors, $\Delta^*_{63\text{-}47}$ and $\Delta^*_{64\text{-}48}$, agree with experimental data. Conclusions: We show that accurate determination of paired Δ_{47} and Δ_{48} is possible using both equilibrated gas and carbonate-based standardization methods. We report new equilibrium Δ_{47} vs Δ_{48} regressions that can be used to identify kinetic effects and quantify biases that may affect temperature reconstructions from unknown samples and constrain regression-based acid digestion fractionation factors.

Equilibrated gas and carbonate standard-derived paired clumped isotope (Δ_{47} and Δ_{48}) values on the absolute reference frame

Rapid Communications in Mass Spectrometry

Jamie K. Lucarelli[1], Hannah M. Carroll[1], Ben M. Elliott[1], Robert A. Eagle[1], Aradhna Tripati[1]

[1]Department of Earth, Planetary, and Space Sciences, Department of Atmospheric and Oceanic Sciences, Institute of the Environment and Sustainability, Center for Diverse Leadership in Science, UCLA, Los Angeles, CA 90095 USA.

Correspondence to: jklucarelli@gmail.com and atripati@g.ucla.edu

Running Head: Robust Methods for Paired Carbonate Clumped Isotope Analysis (Δ_{47} and Δ_{48}) via IRMS

Rationale: Carbonate clumped isotope geochemistry has primarily focused on mass spectrometric determination of mass-47 CO_2 for geothermometry, but theoretical calculations indicate paired analysis of the mass-47 (^{13}C-^{18}O-^{16}O) and mass-48 (^{12}C-^{18}O-^{18}O) isotopologues (denoted with Δ_{47} and Δ_{48} notation) can be used to study non-equilibrium isotope fractionations and refine temperature estimates. We are one of two labs currently utilizing paired Δ_{47} and Δ_{48} measurements to study equilibrium and kinetic isotope effects in carbonates. Additional work is needed on different instruments to define standard Δ_{48} values against equilibrated gases and evaluate Δ_{48} values using carbonate transfer functions.

Methods: We determined Δ_{47} and Δ_{48} of standards using isotope ratio mass spectrometry during the time interval of 2015-2021 on a Thermo Fischer MAT 253 mass spectrometer with a common acid bath digestion system and two Nu Instruments Perspective mass spectrometers with common acid bath and individual reaction vessel digestion systems. A total of 5,581 Δ_{47} and 4,212 Δ_{48} measurements of carbonates, and 183 Δ_{47} and 195 Δ_{48} measurements of gas standards are used from robust correction intervals over multiple years. We report statistical methods for data screening and quality assurance.

Results: Equilibrated gas-based standard values support the accuracy of the recently proposed Δ_{47} I-CDES reference frame and provide robust constraints on Δ_{48} values for carbonate standards. We provide further constraints on the equilibrium Δ_{47} vs Δ_{48} relationship and report values of Devils Hole cave calcite. We demonstrate regression-based acid digestion fractionation factors, $\Delta^*_{63\text{-}47}$ and $\Delta^*_{64\text{-}48}$, agree with experimental data.

Conclusions: We show that accurate determination of paired Δ_{47} and Δ_{48} is possible using both equilibrated gas and carbonate-based standardization methods. We report new equilibrium Δ_{47} vs Δ_{48} regressions that can be used to identify kinetic effects and quantify biases that may affect temperature reconstructions from unknown samples and constrain regression-based acid digestion fractionation factors.

INTRODUCTION

Equilibrium fractionations of multiply heavy isotope substituted isotopologues of $CaCO_3$ have resolvable differences in their relative zero-point energies that are directly related to mineral formation temperature.[1, 2] This relationship is the basis for carbonate clumped isotope thermometry which uses isotope ratio mass spectrometers to measure the frequency with which rare, heavy isotopes of carbon (^{13}C) and oxygen (^{18}O) in carbonate minerals are bonded to each other (instead of bonded to much more common light isotopes) relative to a stochastic distribution. The focus of carbonate clumped isotope research has been based on carbonate ion groups with a mass of 63, which yields mass-47 CO_2 after acid digestion.[2]

Unlike the more widely used oxygen isotope thermometer[3], mass-47 carbonate clumped isotope thermometry does not depend on the bulk oxygen isotope composition ($\delta^{18}O$) of the water it precipitates from.[2] The unique attributes of carbonate clumped isotope measurements allow the reconstruction of numerous paleo-environmental parameters, including but not limited to land[4] and ocean paleotemperatures[5, 6], paleoelevation[7, 8], and dinosaur body temperature[9], while simultaneously estimating water $\delta^{18}O$. Previous research has shown that kinetic isotope effects observed in speleothems[10] and coral[2, 11] may affect the accuracy of temperature reconstructions, which rely on phenomenological relationships between mineral precipitation temperature and mass-47 CO_2. Other research has shown that deviations from equilibrium may exist in some abiotic and biogenic carbonates.[2, 12, 13, 14, 15, 16]

In 2015, we developed a conceptual framework for the use of paired analysis of multiple clumped isotopologues derived from carbonate minerals to identify equilibrium precipitates, refine temperature estimates, and identify non-equilibrium isotope fractionations and their origins.[14] This work builds on our theoretical calculations of isotopic fractionations in carbonate minerals[17], which we have continued to advance.[18] Other work has utilized this framework to advance theoretical predictions of kinetic isotope effects in DIC and simulate fractionations in carbonate minerals.[19]

Recent improvements in mass spectrometry precision have facilitated the first paired analyses of clumped isotopologues of carbonates in standards[20], and one study quantifying paired isotope ratios in carbonates to examine equilibrium and kinetic effects[21]. This work has focused on measurements of both mass 47 and mass 48 CO_2 isotopologues produced after reacting carbonate minerals with phosphoric acid and analyzing the resulting CO_2 (g) on a gas source isotope ratio mass spectrometer. The mass 48 CO_2 isotopologue is produced on digestion of the lower abundance mass 64 carbonate.[17, 18, 14, 20] The abundance of the ^{13}C-^{18}O-^{16}O and ^{12}C-^{18}O-^{18}O isotopologues is denoted with Δ_{47} and Δ_{48} notation.[22] These are defined as:

$$\Delta_{47} = [(R47_{sample}/R47_{stochastic} - 1) \times 1000 \quad \text{(Equation 1)}$$

$$\Delta_{48} = (R48_{sample}/R48_{stochastic} - 1) \times 1000 \quad \text{(Equation 2)}$$

where Ri is the ratio of i/44 CO_2 isotopologues, and Δ_{47} and Δ_{48} are given in parts per thousand (‰).[2, 23]

The precise measurement of mass 47 CO_2 was enabled by modification of the Thermo MAT 253, specially configured with m/z 47-49 Faraday cups[22] and digestion and purification methods for carbonate minerals[2], with mass-48 and mass-49 used to screen for contaminants. Inter-lab reproducibility of sample Δ_{47} values was advanced by using accurately determined carbonate standard values that are anchored to the absolute reference frame detailed by Dennis et al. (2011), allowing for interlaboratory standardization. Recent work from Bernaconi et al. (2021) has proposed carbonate standard anchor values and presented a proposal for carbonate standardization in the 90 °C reference frame that has been further validated using an extensive dataset[24] from our lab.

Measurements of mass 48 CO_2 have been explored recently due to the use of 10^{13} Ω resistors for m/z 47-49 Faraday cups in the Thermo MAT 253 Plus (used in Fiebig et al., 2019 and Bajnai et al., 2020), and the use of secondary electron suppression in the Nu Perspective IS (used here). These advances both contribute to a robust foundation for determination of Δ_{48} values on the absolute reference frame. The most abundant mass 48 CO_2 isotopologue ($^{12}C^{18}O^{18}O$) has two ^{18}O substitutions and is therefore in extremely low abundance at 4.1 ppm in air, which is an order of magnitude lower than mass 47 isotopologues (45 ppm).[2] The minor mass 48 CO_2 isotopologue ($^{13}C^{18}O^{17}O$) has an abundance of 16.7 ppb.[2]

Due to the low abundance of mass 48 CO_2 isotopologues and potential for analytical error, the development of robust standard values and data quality assurance procedures is critical in ensuring accurate determination of unknown sample Δ_{48}. We represent the second lab using paired Δ_{47} and Δ_{48} measurements for applications to geochemistry. Therefore, building on work that has analytically advanced Δ_{47} [22, 2, 7, 25, 26, 27, 24], along with our conceptual framework for utilizing paired Δ_{47} and Δ_{48} measurements[14] and theoretical calculations[17, 18, 19, 21], and recent experimental contributions to the literature[20, 21], here we use both equilibrated gases and carbonate-based standardization to report Δ_{47} and Δ_{48} values for 27 carbonates, including 23 standards and 4 carbonates from Devils Hole[28, 29, 30, 14], determined on different mass spectrometer configurations over multiple years.

1. EXPERIMENTAL DESIGN

1.1 Overview

Analyses are from 3 mass spectrometers using 5 instrumental configurations (Table 2), with varying acid digestion systems and temperatures, ion beam intensity, integration time, and standardization method. Previous work by Upadhyay et al. (in review) established that Δ_{47} can be

accurately determined with statistically identical values using these mass spectrometer configurations, and we sought to determine if this is possible for the coupled measurement of Δ_{47}-Δ_{48}. We also sought to develop robust statistical methods for quality control that can be employed universally by clumped isotope researchers to further improve accuracy, precision, and inter-lab reproducibility. By analyzing the coupled Δ_{47} and Δ_{48} measurement for standards and comparing experimental data to calcite mineral theoretical equilibrium[17, 14], we constrain the equilibrium Δ_{47} vs Δ_{48} relationship over a large temperature range (0-1000 ºC) and develop regressions for clumped isotope fractionations associated with the phosphoric acid digestion of calcite mineral into CO_2 gas, $\Delta^*_{63\text{-}47}$ and $\Delta^*_{64\text{-}48}$.

For this work, we use extensive multi-year datasets to determine carbonate standard Δ_{47} and Δ_{48} values. We also share R scripts that can be used for data quality control, to eliminate the need for manual identification of replicates that do not meet quality control standards, because the latter requires considerable time and expertise to perform on large datasets and has the potential to unintentionally introduce bias and human error. We use equilibrated gas data to calculate carbonate standard Δ_{47} and Δ_{48} values. Our findings validate the accuracy of Δ_{47} values from Bernasconi et al. (2021) and Upadhyay et al. (in review). We provide values for Δ_{48} for a suite of standards, including those reported in Fiebig et al. (2019) and Bajnai et al. (2020), and for additional standards and Devils Hole vein calcite.

We used equilibrated gas based Δ_{47} and Δ_{48} values as anchors to construct carbonate-based transfer functions for additional carbonate standards, instead of equilibrated CO_2 gas-based transfer functions. Our work confirms the applicability of carbonate-based standardization for determination of Δ_{48} across three instrument configurations because it replicates Δ_{48} values for consistency standards (standards not used in slope corrections or transfer functions).

We show that robust standardization with multiple years of data also has the potential to improve the empirically derived Δ_{47}-Δ_{48} equilibrium relationship. We calculate the Δ_{47} and Δ_{48} equilibrium relationship between 0-1000 ºC based on a combination of experimental data, theoretical calcite mineral clumped isotope equilibrium from Hill et al. (2014) and Tripati et al. (2015), and calculated regressions for the calcite-CO_2 acid digestion fractionation factors, $\Delta^*_{63\text{-}47}$ and $\Delta^*_{64\text{-}48}$.

1.2 Carbonates analyzed

In total, 27 different carbonates were analyzed for clumped and bulk isotope compositions. See Table 1 for a description of the mineralogy and origin of all carbonates, modified from Upadhyay et al. (in revision). These particular materials were chosen for analysis because 1) many of them are standards used widely among clumped isotope labs, such as the ETH standards and Carrara Marble, 2) they are used commonly in a certain region or country, such as ISTB-1, TB-1, and TB-2, which are clumped isotope standards from the China University of Geosciences, 3) this suite of standards encompasses numerous biogenic and synthetic standards, 4) the materials are presumed to have near equilibrium clumped isotope

values, such as Devils Hole, ETH-1, and ETH-2, and 5) many analyses (n > 50) were available to provide robust standard values to further constrain Δ_{47} and Δ_{48} on the absolute reference frame.

2. METHODS

We determined coupled Δ_{47}-Δ_{48} values for 24 carbonates and standards, and Δ_{47} values alone for 27 carbonates including standards, on five mass spectrometer configurations at the Tripati Lab, University of California, Los Angeles. This was done in a multi-step process. We first used Config. 1a (Table 2) to determine the $\Delta_{47\ CDES\ 90}$ and $\Delta_{48\ CDES\ 90}$ values of 8 standards using standardization based on 25 ºC and 1000 ºC equilibrated gases. The $\Delta_{47\ CDES\ 90}$ values determined for ETH 1, ETH-2, ETH-3, and ETH-4 were in good agreement with the multi-lab determined nominal values in Bernasconi et al. (2021) (See Results Table 3). We then used the nominal $\Delta_{47\ CDES\ 90}$ values for ETH 1, ETH 2, and ETH 3 from Bernasconi et al. (2021) in combination with two additional carbonate standards as anchors (see following section) for carbonate-based standardization on four additional mass spectrometer configurations, Configs. 1b, 1c, 2, 3 (Table 2). The $\Delta_{48\ CDES\ 90}$ values determined on Config. 1a with gas-based standardization for ETH-1, ETH-2, and ETH-3 with additional carbonate standards were used as anchor values on Configs. 1b, 1c, 2 and 3 for carbonate-based standardization.

2.1 Equilibrated gas standards

For Config. 1a (Nu Instruments Perspective), equilibrated gases were used to allow for projection into the Δ_{47} absolute reference frame at 90 ºC [25], $\Delta_{47\ CDES\ 90}$, and projection into the Δ_{48} absolute reference frame at 90 ºC, $\Delta_{48\ CDES\ 90}$.[20] We have utilized two gases with differing bulk isotope values, with a ~60 ‰ difference in δ_{47}. The depleted δ_{47} gas is from an Airgas CO_2 gas cylinder and was equilibrated with 5-10 mL of 25 ºC deionized (DI) water. The enriched δ_{47} gas is produced by phosphoric acid digestion of a Carrara Marble carbonate standard. The produced carbon dioxide was equilibrated with evaporated DI water held at 25 ºC. Aliquots of the two 25 ºC gases are re-equilibrated at 1000 ºC by heating the gases in quartz tubes inside a muffle furnace for >1 hour, and then flash cooled, to produce gases with near stochastic Δ_{47} values.

2.2 Carbonate Standards

2.2.a. Carbonate standards used as anchors for transfer functions

We used a suite of "anchor" standards in transfer functions to project our data into the Δ_{47} Intercarb Carbon Dioxide Equilibrium Scale (I-CDES)[27] in the 90 ºC absolute reference frame, $\Delta_{47\ I\text{-}CDES}$ (see Methods section 2.5.d). Standards used as $\Delta_{47\ I\text{-}CDES}$ anchors for Config. 1b, 1c, 2, and 3 were ETH-1 (n = 767), ETH-2 (n = 726), and ETH-3 (n = 463). These standards were used as anchors because they have very different bulk isotope compositions (see Supplementary Table

S15), thereby allowing for adequate linearity and scale compression corrections (see Methods section 2.5); are widely available; have been routinely analyzed in our lab since 2014; and their nominal $\Delta_{47\ \text{I-CDES}}$ values were determined by comparing the data from 25 mass spectrometers in 22 laboratories.[27] Config. 2 used two additional anchors, Carmel Chalk (n = 640) and Veinstrom (n = 728), whose $\Delta_{47\ \text{I-CDES}}$ values had been previously determined in this study on Configs. 1b, and 3. These two standards have also been routinely analyzed in our lab since 2015.

Anchor standards were also used to project standard data into the Δ_{48} Carbon Dioxide Equilibrium Scale (CDES) in the 90 ºC absolute reference frame, $\Delta_{48\ \text{CDES}\ 90}$ [20](see Methods 2.5.c and 2.5.e). The standards used as $\Delta_{48\ \text{CDES}\ 90}$ anchors for Config. 1b, 1c, and 2 were ETH-1 (n = 464), ETH-2 (n = 439), and ETH-3 (n = 236). Config. 2 used one additional anchor standard, Veinstrom (n = 436), whose $\Delta_{48\ \text{CDES}\ 90}$ value was previously determined on Configs. 1a and 1b.

Typically, 4-5 anchor standards are analyzed with 5 unknown samples. Robustly determined anchor standards Δ_{47} and Δ_{48} are used to create transfer functions used to determine unknown sample $\Delta_{47\ \text{I-CDES}}$ and $\Delta_{48\ \text{CDES}\ 90}$ (see Methods 2.5).

2.2.b. Consistency standards

We used a suite of "consistency" standards, whose values were treated as unknowns, to ensure reproducibility across mass spectrometer configurations. The $\Delta_{47\ \text{I-CDES}}$ consistency standards used for comparison between Configs. 1b, 2, and 3 were Carrara Marble and ETH-4. Additional $\Delta_{47\ \text{I-CDES}}$ consistency standards used for comparison between Configs. 2 and 3 were CM Tile, IAEA-C1, IAEA-C2, and Merck. Additional $\Delta_{47\ \text{I-CDES}}$ consistency standards used for comparison between Configs. 1 and 3 were Carmel Chalk and TV03.

The $\Delta_{48\ \text{CDES}\ 90}$ consistency standards used for comparison between Configs. 1b and 2 were Carmel Chalk, Carrara Marble, CM Tile, and ETH-4.

2.2.c. Additional carbonate standards

These standards were analyzed either on only one mass spectrometer configuration or their value was averaged from more than one configuration because of n < 9 (see Section 3.2) replicates per configuration. The additional standards include SRM 88b, 102-GC-AZ01, 47407 Coral, ISTB-1, Mallinckrodt, NBS-19, Spel 2-8-E, TB-1, TB-2, and TV01.

2.3. Devils Hole vein calcite

Four samples of vein calcite from Devils Hole (DH) core 2, Amargosa Desert, Nevada were analyzed for $\Delta_{47\ \text{I-CDES}}$ and $\Delta_{48\ \text{CDES}\ 90}$. Devils Hole calcite is assumed to have precipitated near isotopic equilibrium due to an extremely slow precipitation rate (0.1-0.8 μm year^{-1}), low calcite saturation index (0.16-0.21) and a stable temperature of 33.7 (±0.8) ºC throughout the Holocene.[28, 29, 30, 14] DH samples were analyzed for use in the construction of a Δ_{47}-Δ_{48}

equilibrium relationship, and in the determination of the acid digestion fractionation factors from calcite mineral to CO_2 gas, $\Delta^*_{63\text{-}47}$ and $\Delta^*_{64\text{-}48}$. The DH samples reported here are from sections 10 (172 ± 4 ka), 11 (163 ± 4 ka), 12 (157 ± 5 ka), and 13 (151 ± 5 ka)[31] of core 2.

2.4 Instrumentation

Standards and unknowns were analyzed on 3 mass spectrometers using 5 configurations (Table 2). Configs. 1a, 1b, 1c and 2 use Nu Instruments Perspective isotope ratio mass spectrometers (IRMS). Configs. 1a, 1b, and 1c use the same mass spectrometer with differences in the acid digestion system, ion beam intensity, integration time, and mode of standardization detailed in Table 2. The most notable difference between Nu Instruments Perspective and the more widely used Thermo Fisher MAT 253 is the use of secondary electron suppression carried out by two curved plates with a voltage difference in front of the Faraday collectors for m/z 47-49. This advancement has contributed to a Δ_{47} non-linearity slope for the Nu Perspective (median slope observed was -0.00005) that ranges from one to two orders of magnitude less than the MAT 253 (median slope observed was -0.007), and a Δ_{48} non-linearity slope for the Nu Perspective (median slope observed was -0.004) that is an order of magnitude less than the MAT 253 (median slope observed was -0.013). The resulting improvements in accuracy and precision enabled the Nu Perspective mass spectrometers to yield reproducible Δ_{48} data, while the Δ_{48} data produced on the MAT 253 may only be applicable in some situations, such as examining for disequilibrium signals or screening for sample contamination (see Results).

Config. 1a, 1b, and 1c use an in-house constructed autosampler that is similar to the setup detailed in Passey et al. (2010). The configuration uses a stainless steel Costech Zero Blank autosampler, a 105 wt% phosphoric acid bath that digests calcium carbonate samples at 90 °C. The sample gas passes through cryogenic purification traps that use dry ice-cooled ethanol and liquid nitrogen to remove contaminant gases that have low vapor pressure, mostly consisting of water vapor. The CO_2 gas then passes through elemental silver wool (Sigma-Aldrich) to remove sulphur compounds, followed by a gas chromatograph (GC) column with helium carrier gas that contains Porapak Type-Q™ 50/80 mesh column packing material to remove organic compounds. The GC column is maintained at a constant temperature of -20 °C during sample purification. Large samples (4-7 mg) are analyzed in bellows with 4 passes of 20 cycles yielding 80 cycles of sample-standard comparison, with a total integration time of 1600 seconds. Small samples (0.5 mg) are analyzed in microvolume mode, with 3 blocks of 20 cycles, with a total integration time of 1200 seconds. The sample and working gas volumes are depleted in microvolume mode at precisely matched rates, with m/z 44 ranging from 80-30 nA during sample acquisition. The sample preparation system is operated by custom software in Labview that controls the sampler, GC column, cryogenic dewar lifters, and valves. The Labview software is integrated with the Perspective Stable Gas Control software interface that controls the Nu Perspective mass spectrometer.

Config. 2 uses a Nu Carb Sample Digestion System instead of a common acid bath, where 0.40-0.60 mg of calcium carbonate were reacted at 70 °C in individual glass vials with 105 wt% phosphoric acid. This eliminates the use of a common acid bath. The sample gas is cryogenically purified in liquid nitrogen-cooled tubes called coldfingers before passing into a relatively short GC column packed with Porapak Type-Q™ 50/80 and silver wool. This instrument operates under vacuum pressure and does not use a carrier gas. The sample and working gas volumes are matched precisely during depletion into the mass spectrometer. Sample data is analyzed in three blocks of 20 cycles, with each cycle integrating for 20 seconds, for a total integration time of 1200 seconds.

Raw data is transferred into Easotope 64-bit version from release 20201231, where all corrections are calculated. All data uses the IUPAC parameter set.[32, 33]

2.5 Corrections applied to raw Δ_{47} and Δ_{48}

2.5.a Gas standard based slope corrections

On Config. 1a, a combined slope was determined over a 10-day moving average for the regression lines $\delta_{47\ raw}$ vs $\Delta_{47\ raw}$ and $\delta_{48\ raw}$ vs $\Delta_{48\ raw}$ for CO_2 gas standards equilibrated at 25 °C and 1000 °C (Figure 1a, b). The determination of this slope demonstrated the correlation between $\delta_{47\ raw}$ vs $\Delta_{47\ raw}$ and $\delta_{48\ raw}$ and $\Delta_{48\ raw}$. Slope corrections are applied to all samples using Equations 3 and 4

$$\Delta_{47\ sc} = \Delta_{47\ raw} - (m_{47} \times \delta_{47\ raw}) \quad \text{(Equation 3)}$$

$$\Delta_{48\ sc} = \Delta_{48\ raw} - (m_{48} \times \delta_{48\ raw}) \quad \text{(Equation 4)}$$

where $\Delta_{47\ sc}$ and $\Delta_{48\ sc}$ are the slope corrected $\Delta_{47\ raw}$ and $\Delta_{48\ raw}$, and m_{47} and m_{48} are the gas line regression slopes, with nomenclature adapted from Fiebig et al. (2019). The gas standard based slope corrections for all standards can be found in Supplementary Tables S1 and S2.

2.5.b Carbonate standard-based slope corrections

For Configs. 1b, 1c, 2, and 3, ETH-1 and ETH-2 were used to determine 10-day moving average slopes for the regression lines $\delta_{47\ raw}$ vs $\Delta_{47\ raw}$ and $\delta_{48\ raw}$ vs $\Delta_{48\ raw}$ (Figure 1c-h). The slopes were then used in Equations 3 and 4 to determine the slope corrections for all samples. The carbonate standard based slope corrections for all standards can be found in Supplementary Tables S3-S14.

2.5.c Δ_{47} and Δ_{48} in the CDES 90 reference frame using gas standard based standardization

For Config. 1a, $\Delta_{47\ sc}$ and $\Delta_{48\ sc}$ were projected into the Carbon Dioxide Equilibrium Scale[4] in the 90 °C absolute reference frame (CDES 90), using methods detailed in Dennis et al. (2011) and nomenclature adapted from Fiebig et al. (2019). The 10-day moving average slope and intercept was determined for the linear relationship between theoretically calculated Δ_{47} values for 25 °C and 1000 °C, 0.925 ‰ [34] and 0.027 ‰ [25], respectively, vs measured $\Delta_{47\ sc}$. This was also done for theoretically calculated Δ_{48} values for 25 °C and 1000 °C of 0.345 ‰ [34] and 0.000 ‰ [20], respectively, vs measured $\Delta_{48\ sc}$. The equilibrated gas transfer function (EGTF) slope and intercept from these regressions were used to create empirical transfer functions, which are applied to all $\Delta_{47\ sc}$ and $\Delta_{48\ sc}$ values on Config. 1a, and yields the fully corrected values $\Delta_{47\ CDES\ 90}$ and $\Delta_{48\ CDES\ 90}$, using equations 5 and 6

$$\Delta_{47\ CDES\ 90} = \Delta_{47\ sc} \text{ x EGTF slope} + \text{EGTF intercept} \qquad \text{Equation 5}$$

$$\Delta_{48\ CDES\ 90} = \Delta_{48\ sc} \text{ x EGTF slope} + \text{EGTF intercept} \qquad \text{Equation 6}$$

where $\Delta_{47\ CDES\ 90}$ and $\Delta_{48\ CDES\ 90}$ are the fully corrected values digested in phosphoric acid at 90 °C, $\Delta_{47\ sc}$ and $\Delta_{48\ sc}$ are the slope corrected values from Equations 3 and 4, EGTF slope is the equilibrated gas transfer function slope, and EGTF intercept is the equilibrated gas transfer function intercept. We have chosen to omit the acid fractionation factor (AFF) correction that is historically used to transfer fully corrected 90 °C values into the 25 °C reference frame, $\Delta^*_{47\ 90\text{-}25}$, to avoid the additional error potentially associated with this transformation, given that $\Delta^*_{47\ 90\text{-}25}$ is poorly constrained and there is currently no known $\Delta^*_{48\ 90\text{-}25}$. All gas-standard based empirical transfer function slopes and intercepts are in Supplementary Tables S1 and S2.

2.5.d Δ_{47} in the I-CDES reference frame

For Configs. 1b, 1c, 2 and 3, carbonate-based transfer functions were used instead of equilibrated gas-based transfer functions. We have chosen to use the newly developed Intercarb-Carbon Dioxide Equilibrium Scale (I-CDES) reference frame, $\Delta_{47\ I\text{-}CDES}$, which was developed after comparing the data from 25 mass spectrometers in 22 laboratories to determine nominal carbonate standard values for ETH-1, ETH-2, and ETH-3 for use in transferring data into the absolute reference frame.[27] I-CDES is in the 90 °C reference frame, which omits the practice of transferring final data into the 25 °C reference frame and the associated error, and potentially increases inter-lab reproducibility by using well-constrained $\Delta_{47\ I\text{-}CDES}$ values for widely available carbonate standards (ETH-1, ETH-2, ETH-3) as "anchors" for corrections. Our long-term ETH-1, ETH-2, and ETH-3 values determined with equilibrated gas corrections (Table 3) support the new nominal anchor values from Bernasconi et al (2021). $\Delta_{47\ I\text{-}CDES}$ values of 0.2052, 0.2085, and 0.6132 were used as "known" anchor values for ETH-1, ETH-2, and ETH-3, respectively, for transfer functions.[27]

The 10-day moving average slope and intercept was determined for the linear relationship between the ETH-1, ETH-2, and ETH-3 $\Delta_{47\ I\text{-}CDES}$ anchor values vs the $\Delta_{47\ SC}$ values. To create our carbonate standard based transfer functions (CSTF) applied to all standards and unknown samples, the slope and intercept from these regressions are used in Equation 7

$$\Delta_{47\ I\text{-}CDES} = \Delta_{47\ sc} \text{ x CSTF slope} + \text{CSTF intercept} \qquad \text{Equation 7}$$

where $\Delta_{47\ I\text{-}CDES}$ is the fully corrected value in the I-CDES reference frame at 90 ºC, $\Delta_{47\ sc}$ is the slope corrected value from equation 3, CSTF slope is the carbonate standard transfer function slope, and CSTF intercept is the carbonate standard transfer function intercept. All Δ_{47} CSTF slopes and intercept are available in Supplementary Tables S3, S5, S7, S9, S11, and S13.

Config. 2 uses the same method detailed above with the additional standards Carmel Chalk and Veinstrom used as anchors for transfer functions. The "known" anchor $\Delta_{47\ I\text{-}CDES}$ values used for Carmel Chalk and Veinstrom were 0.674 and 0.715, respectively. Before Carmel Chalk and Veinstrom were used as anchors in Config. 2, their "known" values were determined in the I-CDES reference frame as long term combined instrument averages for Configs. 1b and 3 using the method described above.

2.5.e Δ_{48} in the CDES 90 reference frame using carbonate standard based corrections

$\Delta_{48\ CDES\ 90}$ standard values determined on Config. 1a using equilibrated gas corrections (see Results Table 4) were used as "known" anchor values on Configs. 1b, 2, and 3 to calculate carbonate standard based transfer functions. Configs. 1b, 2, and 3 all used ETH-1, ETH-2, and ETH-3 as anchors, Config. 2 used Veinstrom as an additional anchor, and Config. 3 used Carrara Marble and Veinstrom as additional anchors. The 10-day moving average slope and intercept was determined for the linear relationship between the $\Delta_{48\ CDES\ 90}$ anchor values vs the $\Delta_{48\ sc}$ values. To create the carbonate standard transfer function (CSTF) that is applied to all standards and unknown samples, the slope and intercept from these regressions are used in equations 8,

$$\Delta_{48\ CDES} = \Delta_{48\ sc} \text{ x CSTF slope} + \text{CSTF intercept} \qquad \text{Equation 8}$$

where $\Delta_{48\ CDES\ 90}$ is the fully corrected value in the CDES 90 reference frame, $\Delta_{48\ sc}$ is the slope corrected value from equation 4, CSTF slope is the carbonate standard transfer function slope, and CSTF intercept is the carbonate standard transfer function intercept. All Δ_{48} CSTF slopes and intercept are available in Supplementary Tables S4, S6, S8, S10, S12, and S14.

2.6 Use of statistical methods for robust determination of Δ_{47} and Δ_{48}

Statistical analyses were performed in R version 4.0.4 [35]. R code and raw data used in analyses are publicly available for review at https://github.com/Tripati-Lab/Lucarelli-et-al. Following acceptance for publication, code and raw data will be permanently archived on Dryad, a static link will be provided, and this section will be updated.

2.6.a Statistical techniques used for data quality assurance

We use a new statistical technique for Δ_{47} and Δ_{48} quality assurance. For each standard of interest, we calculated a kernel density estimate using the generic S3 method 'density' included in base R's stats package.[35] Kernel density estimation is a nonparametric probability density method akin to a histogram with an added smoothing parameter. A nonparametric approach is preferred because we often have no *a priori* knowledge of the statistical properties of the raw clumped isotope replicate pool. The kernel used in density estimates is a weighting function; in the R implementation, the default is to use a normally distributed (Gaussian) kernel, K, applied to a variable, u.[35] The standard normal distribution takes the form:

$$K(u) = \frac{1}{\sqrt{2\pi}} e^{-\frac{1}{2}u^2}$$

The smoothing parameter, known as bandwidth, using the default normally distributed kernel, is set to equal the standard deviation of the kernel itself.[35] The kernel then becomes a curve that integrates to 1 with the statistical properties:

$$\sigma^2(K) = t^2 K(t)\, dt$$

For a full explanation of bandwidth selection in nonparametric probability density estimation, see Sheather & Jones (1991); for a full explanation of kernel density estimation as implemented in R, see Deng & Wickham (2011).[36, 37]

Kernel density estimation is used to examine the underlying probability density function (PDF) for a given variable. Each measured clumped isotope value is not a single definite point, due to the uncertainty inherent in measurement, but is rather a finite probable range of values. This can be visualized as a peak where the most probable values for a given variable cluster together to produce the peak's maxima. From the PDF peak for each standard, we found the nearest minima on either side of the maxima and defined those as the initial cutpoints for exclusion of poorly constrained data (Figure 2b). In cases where the PDF revealed a double peak or a shoulder at least a third as high as the true maxima, we used the second nearest minima or left/right minima according to the shape of the density peak. These cases are fully described in Supporting Information Appendix A, along with a guide to the quality control and data screening process. The density-based minima exclusion method has been included as a custom function in the accompanying R script, Supporting Information Appendix B, and instructions for its use are

given in the script. Hereafter, we refer to this statistical technique as the "nearest minima method" for the sake of brevity.

Following initial exclusions based on the nearest minima, we employed a 3σ exclusion. A Shapiro-Wilk test was used to determine whether the resulting data were normally distributed. If the Shapiro-Wilk test indicated non-normality, cuts at either 2σ or 1σ were used as needed to obtain normally distributed data. In the comparatively rare case where normally distributed final data were not obtainable with any cut, the cut was chosen to maximize the W statistic of the Shapiro-Wilk test. Throughout, we report the final cut used and whether the final data are normally distributed. A visual representation of the data at each step in this process is included in Figure 2. Means determined using this statistical approach are consistent with what we report elsewhere for a different set of data analyses for Δ_{47} [24], and the more time-consuming traditional analysis we performed for both Δ_{47} and Δ_{48} during data exploration for this study.

2.6.b Inter-instrumental comparisons

Five mass spectrometer configurations, as described in section 2.4 and Table 2, were used to measure clumped isotopes in this study. Replicate data from each configuration were excluded independently of one another using the nearest minima method described in section 2.6.a. To test for any measurement differences between configurations that would preclude pooling data for analyses, we modeled final clumped isotope values by the additive effects of configuration and standard using a linear mixed effects model from package *nlme* version 3.1-152.[38] The standard error of the final clumped isotope value was included as a random effect in the model. Models did not include carbonates which are run only rarely on our instrumentation, and for which we have few replicates. These were ISTB-1, TB-1, TB-2, CIT Carrara, DH-2-10, DH-2-11, DH-2-12, DH-2-13, TV01, 47407 Coral, Spel-2-8-E, and 102-GC-AZ01. Pairwise differences between configurations were then assessed using contrasts with adjustment for multiple comparisons from package *emmeans* version 1.5.4.[39] Estimated marginal means are preferred to ordinary marginal means because they control for differences in the number of analyses run on individual configurations, *i.e.*, a configuration running more standards overall, or more replicates of a particular standard, is not given more weight in the pairwise analysis than one running fewer.

Data were pooled for further analyses only if there was no evidence of a statistically significant difference between configurations across any of the standards reported herein. For Δ_{48}, Config. 3 was not pooled with Configs. 1b and 2 because offsets were observed in anchor standards ETH-1 and ETH-2 (known equilibration temperature of 600 ºC) that did not exist in Configs. 1b and 2 (see Table 7). Config. 3 is a Thermo Finnigan MAT 253 and does not use secondary electron suppression, and therefore, may not yield as precise Δ_{48} data as Configs. 1 and 2 which are Nu Instruments Perspective mass spectrometers with secondary electron suppression (see section 2.4). Additionally, a power analysis indicated that Config. 3 requires >4x the amount of replication than Configs. 1b and 2 to reach a long-term mean (see the following section and Results section 3.2).

2.6.c Power analysis

We employed power analysis to determine the number of replicates needed to reach the overall mean for Δ_{47} and Δ_{48}. This was accomplished via the two-sample t-test power function in package pwr version 1.3-0.[40] Cohen's d was populated with the overall mean and standard deviation of the final, quality-controlled dataset for each standard, power was set to 0.95, and the significance level, α, set to 0.05. The number of required replicates was averaged over standards to produce recommendations for replication. We excluded standards for which the recommended number of replicates was greater than the number of replicates included in our dataset. Sample replicate recommendations should be interpreted as the typical minimum number of replicates needed after the exclusion of poorly constrained replicates via the nearest minima method described in section 2.6.a.

3. RESULTS AND DISCUSSION

3.1 Instrument comparison

We found no evidence of statistically significant differences in final clumped isotope values between configurations for either $\Delta_{47\ \text{I-CDES}}$ or $\Delta_{48\ \text{CDES 90}}$. See Supplementary Table S16 and Fig. S1 for pairwise configuration comparisons for $\Delta_{47\ \text{I-CDES}}$ analyses. See Supplementary Table S17 and Fig. S2 for pairwise configuration comparisons for $\Delta_{48\ \text{CDES 90}}$ analyses. Config. 1a used gas-standard based standardization while Configs. 1b and 2 used carbonate standard based standardization. We therefore present $\Delta_{48\ \text{CDES 90}}$ analyses for Config. 1a individually, while Configurations 1b and 2 were pooled for analyses. Config. 3 is an older generation mass spectrometer which does not have secondary electron suppression, possibly leading to decreased precision when measuring the relatively low abundance m/z 48 CO_2 isotopologue and was not pooled with Configs. 1b and 2. All other analyses were produced by a single configuration or were measured too rarely to be included in the overall inter-instrumental comparison.

3.2 Power analysis

Power analysis was used to determine the number of replicates necessary to achieve the overall mean for a given standard with 95% power and an α of 0.05. Replicate recommendations are to be understood as the final pool of replicates per standard after elimination of replicates identified as poorly constrained via the nearest minima method. See Table 2 for a description of mass spectrometer configurations. Factors that influence the number of required replicates include integration time and ion beam intensity which vary between configurations. Additional time- and condition-dependent factors include signal/noise, instrument stability, linearity corrections, and cleanliness of measured gases, all can influence reproducibility. Therefore, this

analysis shows what is typical given long-term variability, and not necessarily what is characteristic of any given set of intervals for a particular instrument.

For Δ_{47} analyses we found that typically ~14 replicates per standard were needed for Configurations 1b and 3 to become statistically indistinguishable from the long-term mean. Approximately 3 replicates per standard were needed on Configuration 2. We were not able to reliably determine the number of replicates needed for Configuration 1a.

For Δ_{48} analysis on Configuration 1a, which is standardized with equilibrated gases only, we found that typically ~18 replicates were needed per standard. Configurations 1b and 2, which use carbonate standard-based standardization, typically required ~9 replicates per standard to become statistically indistinguishable from the long-term mean. Configuration 3, which is an older generation mass spectrometer (Thermo Fisher MAT 253) using carbonate-based standardization, typically required ~37 replicates.

3.3 Δ_{47} and Δ_{48} results determined using equilibrated gas-based standardization

$\Delta_{47\ \mathrm{CDES\ 90}}$ values were determined for 8 standards using equilibrated gas-based standardization, with a total of 370 analyses performed from May 2015-August 2016 on Config. 1a (Table 3). All standard replicate data were determined to be normally distributed by Shapiro-Wilk normality tests, with the exception of heated gas (Supplementary Table S18). The long-term average $\Delta_{47\ \mathrm{CDES\ 90}}$ values for ETH-1, ETH-2, and ETH-3 were within 1 standard error of the nominal anchor values determined in Bernasconi et al. (2021) (Figure 3, Table 3). The largest $\Delta_{47\ \mathrm{CDES\ 90}}$ offset observed between the two datasets is 0.012 for ETH-4. The offset is still within 1 SD and ETH-4 is not used as an anchor standard.

$\Delta_{48\ \mathrm{CDES\ 90}}$ values were determined for 8 standards using equilibrated gas-based standardization, with a total of 434 analyses performed from May 2015-June 2017. All replicate data were normally distributed (Table S19). Currently, the other published $\Delta_{48\ \mathrm{CDES\ 90}}$ data using only equilibrated gas-based corrections is from Feibig et al. (2019). The $\Delta_{48\ \mathrm{CDES\ 90}}$ values for ETH-1, ETH-2, and ETH-3 from this study and Fiebig et al. (2019) are within 1 SE, while ETH-4 and Carrara Marble are within 2 SE (<1 SD) (Figure 4, Table 4).

3.4 Δ_{47} and Δ_{48} results determined using carbonate-based standardization

$\Delta_{47\ \mathrm{I\text{-}CDES}}$ values were determined for 27 carbonate standards using carbonate standard-based slope corrections and transfer functions, with a total of 5211 analyses performed from April 2015-March 2021 on Configs. 1b, 1c, 2, and 3 (Table 5). All standard replicate data were determined to be normally distributed, with the exception of ETH-3 on Config 3 (Supplementary Table S20). We used IAEA-C1, IAEA-C2, Merck, and ETH-4 as consistency standards (they were not used as anchors) for direct comparability to Bernasconi et al. (2021). The long term combined instrument average for IAEA-C1, IAEA-C2, and Merck were within 1 SE, and ETH-4 was within <1 SD of values determined in Bernasconi et al. (2021) (Figure 5, Table 6), which

were determined with the combined data from 22 laboratories. Configs. 1b, 1c, 2, and 3 produced $\Delta_{47\ \text{I-CDES}}$ replicate data that was statistically indistinguishable (Supplementary Table S16).

$\Delta_{48\ \text{CDES 90}}$ values were determined for 24 carbonate standards using carbonate standard-based slope corrections and transfer functions, with a total of 3113 analyses performed from April 2015-August 2020 on Config. 1b, 1c, and 2 (Table 7). All standard replicate data was determined to be normally distributed except for ETH-1 on Config. 3 (Supplementary Table S19). Currently, the only other available dataset with $\Delta_{48\ \text{CDES 90}}$ data determined using carbonate-based standardization is from Bajnai et al. (2020). The $\Delta_{48\ \text{CDES 90}}$ data for ETH-1, ETH-2, ETH-3 from this study and Bajnai et al. (2020) have differences of -0.010, -0.006, and -0.052, respectively (Figure 6, Table 8). The comparatively large offset observed in the ETH-3 $\Delta_{48\ \text{CDES 90}}$ may be due to more replicates available in this study, or variations in standardization, such as differing carbonate anchor values. However, the large offset is not observed in ETH-3 Δ_{47}, as values have a difference of 0.006 despite this study being in the I-CDES reference frame and Bajnai et al. (2020) using the CDES 90 reference frame.

The Devils Hole calcite vein samples from this study and Bajnai et al. (2020) are from Core DH-2, but from different sections. This study analyzed sections 10 (172+/- 4 ka), 11 (163 +/- 5 ka), 12 (57 +/- 5 ka), and 13 (151 +/- 4 ka)[31], while Bajnai et al. (2020) analyzed section 8 (4.5-16.9 kya). The $\Delta_{47\ \text{I-CDES}}$ replicate values for our 4 DH samples were statistically indistinguishable and were pooled into the Devils Hole Core 2 average, DH-2 average. Our DH-2 average $\Delta_{47\ \text{I-CDES}}$ value of 0.566 (n = 74) has an offset of -0.009 from the DH-2-8 $\Delta_{47\ \text{CDES 90}}$ value of 0.575 (n = 5) from Bajnai et al. (2020) (Figure 6, Table 8).

3.5 $\Delta^*_{63\text{-}47}$ and $\Delta^*_{64\text{-}48}$ acid digestion fractionation factor regressions

Model data from Guo et al. (2009) predicted that acid digestion fractionation factors (AFF) for when calcite mineral is digested in phosphoric acid, $\Delta^*_{63\text{-}47}$ and $\Delta^*_{64\text{-}48}$, would depend on the Δ_{63} and Δ_{64} of the reactant carbonate, respectively. To calculate this dependence, nonlinear regressions of the theoretical model equilibrium Δ_{63} and Δ_{64} vs temperature[17, 14] were used to determine theoretical equilibrium Δ_{63} and Δ_{64} for the precipitation temperature of Devils Hole vein calcite at 33.7 ºC ($\Delta_{63} \approx 0.3707$; $\Delta_{64} \approx 0.1092$). Model equilibrium Δ_{63} and Δ_{64} at 600 ºC ($\Delta_{63} \approx 0.0179$; $\Delta_{64} \approx 0.0022$) was used for ETH-1 and ETH-2. The experimentally determined $\Delta_{47\ \text{I-CDES}}$ values for the four Devils Hole samples from Core DH-2 were statistically indistinguishable and therefore their $\Delta_{47\ \text{I-CDES}}$ (n = 74) and $\Delta_{48\ \text{CDES 90}}$ (n = 76) values were pooled into Devils Hole core 2 average, DH-2. DH-2 and the combined averages of ETH-1/ETH-2 $\Delta_{47\ \text{I-CDES}}$ and $\Delta_{48\ \text{CDES 90}}$ were subtracted from the model equilibrium Δ_{63} and Δ_{64} values, respectively, to yield AFFs for calcite at 33.7 ºC ($\Delta^*_{63\text{-}47} = 0.1949$; $\Delta^*_{64\text{-}48} = 0.1308$) and 600 ºC ($\Delta^*_{63\text{-}47} = 0.1881$; $\Delta^*_{64\text{-}48} = 0.1300$) using equations 9 and 10

$$\Delta^*_{63\text{-}47} = \Delta_{47\ \text{I-CDES}} - \Delta_{63} \qquad \text{Equation 9}$$

$\Delta^*_{64\text{-}48} = \Delta_{48\ \text{CDES 90}} - \Delta_{64}$ Equation 10

where $\Delta^*_{63\text{-}47}$ and $\Delta^*_{64\text{-}48}$ are the AFFs. Fiebig et al. (2019) used a similar method to determine AFFs at 600 ºC. Our 600 ºC $\Delta^*_{63\text{-}47}$ and $\Delta^*_{64\text{-}48}$ differed by 0.008 and 0.006, respectively, from the 600 ºC $\Delta^*_{63\text{-}47}$ and $\Delta^*_{64\text{-}48}$ of 0.196 and 0.136 determined in Fiebig et al. (2019). Since the calculation of AFFs relies on the long term ETH-1 and ETH-2 Δ_{47} and Δ_{48} values, the difference in AFFs is equivalent to the difference in the long term combined ETH-1/ETH-2 Δ_{47} and Δ_{48} from this study (ETH-1/ETH-2 $\Delta_{47\ \text{I-CDES}} = 0.206 \pm 0.0006$, n = 1494; $\Delta_{48\ \text{CDES 90}} = 0.132 \pm 0.002$, n = 903) vs Fiebig et al. (2019) (ETH-1/ETH-2 $\Delta_{47\ \text{I-CDES}} = 0.214 \pm 0.005$, n = 37; $\Delta_{48\ \text{CDES 90}} = 0.138 \pm 0.015$, n = 37).

Linear regressions were made using Δ_{63} vs $\Delta^*_{63\text{-}47}$ and Δ_{64} vs $\Delta^*_{64\text{-}48}$ for DH-2 (33.7 ºC) and ETH-1/ETH-2 (600 ºC) (Figure 7 a,b). The slope and intercept from these regressions were used to calculate $\Delta^*_{63\text{-}47}$ and $\Delta^*_{64\text{-}48}$ for 0-1000 ºC (Table 9), using equations 11 and 12.

$\Delta^*_{63\text{-}47} = 0.0193 \times \Delta_{63} + 0.1878$ Equation 11

$\Delta^*_{64\text{-}48} = 0.0077 \times \Delta_{64} + 0.1300$ Equation 12

The relationship between precipitation temperature and $\Delta^*_{63\text{-}47}$, $\Delta^*_{64\text{-}48}$ were determined to be

Equation 13

$$\Delta^*_{63\text{-}47} = [0.1968 \pm (1.805 \times 10^{-5})] - [(6.111 \times 10^{-5}) \pm (5.894 \times 10^{-7})]T + [(1.922 \times 10^{-7}) \pm (4.733 \times 10^{-9})]T^2 - [(2.965 \times 10^{-10}) \pm (1.304 \times 10^{-11})]T^3 + [(1.762 \times 10^{-13}) \pm (1.126 \times 10^{-14})]T^4$$

Equation 14

$$\Delta^*_{64\text{-}48} = [0.1312 \pm (6.955 \times 10^{-6})] - [(1.113 \times 10^{-5}) \pm (2.271 \times 10^{-7})]T + [(4.398 \times 10^{-8}) \pm (1.824 \times 10^{-9})]T^2 - [(7.799 \times 10^{-11}) \pm (5.025 \times 10^{-12})]T^3 + [(5.041 \times 10^{-14}) \pm (4.340 \times 10^{-15})]T^4$$

where temperature is in Celsius, and $r^2 = 0.9999$ and 0.9992 for Equation 13 and 14, respectively (Figure 7 c,d).

The relationship between $\Delta^*_{63\text{-}47}$ and $\Delta^*_{64\text{-}48}$ were determined to be

$\Delta^*_{64\text{-}48} = (0.3964 \pm 0.0033) + (-2.898 \pm 0.0340)\Delta^*_{63\text{-}47} + (7.88 \pm 0.0887)\Delta^{*2}_{63\text{-}47}$ Equation 15

(Figure 7e).

For samples with unknown precipitation temperature, $\Delta^*_{63\text{-}47}$ and $\Delta^*_{64\text{-}48}$ can be calculated using Equations 16 and 17 (Figure 8a, b).

$$\Delta^*_{63\text{-}47} = 0.0190 \times \Delta_{47\ \text{I-CDES}} + 0.1842 \quad \text{Equation 16}$$

$$\Delta^*_{64\text{-}48} = 0.0077 \times \Delta_{48\ \text{CDES 90}} + 0.1290 \quad \text{Equation 17}$$

where $\Delta_{47\ \text{I-CDES}}$ and $\Delta_{48\ \text{CDES 90}}$ are experimentally determined values. Equations 18 and 19 may be used to calculate Δ_{63} and Δ_{64} from $\Delta_{47\ \text{I-CDES}}$ and $\Delta_{48\ \text{CDES 90}}$ (Figure 8c, d, Table 9).

Equation 18

$$\Delta_{63} = (-0.1845 \pm 0.0007) + (0.9839 \pm 0.0078)\Delta_{47\ \text{I-CDES}} + (-0.0121 \pm 0.0299)\Delta_{47\ \text{I-CDES}}^2 + (0.0207 \pm 0.0483)\Delta_{47\ \text{I-CDES}}^3 + (-0.0125 \pm 0.0281)\Delta_{47\ \text{I-CDES}}^4$$

Equation 19

$$\Delta_{64} = (-0.1377 \pm 0.0048) + (1.166 \pm 0.0981)\Delta_{48\ \text{CDES 90}} + (-1.267 \pm 0.7306)\Delta_{48\ \text{CDES 90}}^2 + (4.007 \pm 2.363)\Delta_{48\ \text{CDES 90}}^3 + (-4.645 \pm 2.807)\Delta_{48\ \text{CDES 90}}^4$$

where $\Delta_{47\ \text{I-CDES}}$ and $\Delta_{48\ \text{CDES 90}}$ are experimentally determined values.

The Δ_{63} vs $\Delta^*_{63\text{-}47}$ slope of 0.0193 determined here (Figure 7a) differs by -0.0112 ‰ from the model predicted slope from Guo et al. (2009) of 0.0305. The model calculated the dependence based on carbonates with $\delta^{13}C = 0$ and $\delta^{18}O = 0$, however, this may not be the source of the offset because the slope is only predicted to change by ~0.002 and ~-0.0005 for a 50 ‰ increase in $\delta^{13}C$ and $\delta^{18}O$, respectively.[41] The slope offset may in-part arise from approximations made in the model calculations for isotopologues containing ^{17}O, and uncertainty in the slope determined in this study from the use of only two temperatures.

3.6 Temperature-dependent Δ_{47} vs Δ_{48} equilibrium

Temperature dependent $\Delta_{47\ \text{I-CDES}}$ and $\Delta_{48\ \text{CDES 90}}$ equilibrium, referred to as $\Delta_{47\ \text{I-CDES EQ}}$ and $\Delta_{48\ \text{CDES 90 EQ}}$, were calculated using two methods. The first method combines equilibrium theory from Hill et al. (2014) and Tripati et al. (2015) with experimentally determined $\Delta_{47\ \text{I-CDES}}$ and $\Delta_{48\ \text{CDES 90}}$, with the AFFs described in Results section 3.5. The second method uses only experimentally determined $\Delta_{47\ \text{I-CDES}}$ and $\Delta_{48\ \text{CDES 90}}$ values. Both regressions lie within the 95% confidence interval of each other.

3.6.a Δ_{47} vs Δ_{48} equilibrium combining theory and experimental values

$\Delta_{47\ \text{I-CDES EQ}}$ and $\Delta_{48\ \text{CDES 90 EQ}}$ were calculated using Equations 20 and 21 (Figure 9)

$$\Delta_{47\ \text{I-CDES EQ}} = \Delta_{63} + \Delta^*_{63\text{-}47} \quad \text{Equation 20}$$

$$\Delta_{48\ \text{CDES 90 EQ}} = \Delta_{64} + \Delta^*_{64\text{-}48} \quad \text{Equation 21}$$

where $\Delta^*_{63\text{-}47}$ and $\Delta^*_{64\text{-}48}$ are the values determined in Section 3.5, Table 9, using a combination of calcite mineral equilibrium theory from Hill et al. (2014) and Tripati et al. (2015) with experimentally determined $\Delta_{47\ \text{I-CDES}}$ and $\Delta_{48\ \text{CDES 90}}$ values for Devils Hole vein calcite and combined ETH-1/ETH-2. Devils Hole calcite was used in construction of the coupled clumped isotope relationship because it is assumed to have precipitated near isotopic equilibrium due to extremely slow precipitation rate (0.1-0.8 μm year^{-1}), low calcite saturation index (0.16-0.21) and a stable temperature of 33.7(±0.8) ºC throughout the Holocene.[31, 29, 30] Combined ETH-1/ETH-2 was used because their $\Delta_{47\ \text{I-CDES}}$ and $\Delta_{48\ \text{CDES 90}}$ values were statistically indistinguishable, and both have a known equilibration temperature of 600 ºC.[42] Additionally, samples equilibrated at high temperatures are much less likely to have detectable kinetic biases due to faster exchange of isotopes among isotopologues and decreased time to reach isotopic equilibrium. The $\Delta_{47\ \text{I-CDES EQ}}$ vs $\Delta_{48\ \text{CDES 90 EQ}}$ temperature-dependent equilibrium relationship in Regression A (Figure 9) is given by a second-degree polynomial, Equation 22.

$$\Delta_{48\ \text{CDES 90 EQ}} = 0.1123 + 0\ .01971\ \Delta_{47\ \text{I-CDES EQ}} + 0.364\ (\Delta_{47\ \text{I-CDES EQ}})^2 \quad \text{Equation 22}$$

The equilibrium regression in Equation 22 (Figure 9, Regression A) lies within the 95% confidence band of the experimentally determined regression in Equation 25 (Figure 9, Regression B; see the following section, 3.6.b).

The temperature-dependent equilibrium relationships are described by Equations 23 and 24,

Equation 23

$$\Delta_{47\ \text{I-CDES EQ}} = [0.6646 \pm (0.0009)] - [0.0032 \pm (3.033 \times 10^{-5})]T + [(1.012 \times 10^{-5}) \pm (2.449 \times 10^{-7})]T^2 - [(1.559 \times 10^{-8}) \pm (6.717 \times 10^{-10})]T^3 + [(9.251 \times 10^{-12}) \pm (5.802 \times 10^{-13})]T^4$$

Equation 24

$$\Delta_{48\ \text{CDES 90 EQ}} = [0.2842 \pm (0.0009)] - [0.0014 \pm (3.048 \times 10^{-5})]T + [(5.741 \times 10^{-6}) \pm (2.437 \times 10^{-7})]T^2 - [(1.017 \times 10^{-8}) \pm (6.749 \times 10^{-10})]T^3 + [(6.570 \times 10^{-12}) \pm (5.830 \times 10^{-13})]T^4$$

where temperature is Celsius.

3.6.b Experimentally determined Δ_{47} vs Δ_{48} regression

A second-degree polynomial given by Equation 25 ($r^2 = 0.9726$) was fit through 20 experimentally determined $\Delta_{47\ I\text{-}CDES}$ vs $\Delta_{48\ CDES\ 90}$ values for carbonate standard materials determined in this study (Regression B in Figure 9).

Equation 25

$$\Delta_{48\ CDES\ 90\ EQ} = (0.1179 \pm 0.0266) - (0.0398 \pm 0.1332)\Delta_{47\ I\text{-}CDES\ EQ} + (0.4407 \pm 0.1490)\Delta_{47\ I\text{-}CDES\ EQ}^2$$

All $\Delta_{47\ I\text{-}CDES}$ and $\Delta_{48\ CDES\ 90}$ values used to calculate this regression can be found in Tables 6 and 7, respectively. Of the 21 carbonates in Figure 8, all lie within 1 SE of the 95% confidence interval of Regression B, with the exception of Merck, Carmel Chalk, and 47407 Coral. 47407 Coral was the only sample for which we determined $\Delta_{48\ CDES\ 90}$ and did not include in the regression due to the apparent offset from $\Delta_{48\ CDES\ 90}$ equilibrium. 47407 Coral is a deep-sea coral of the genus *Desmophyllum* with an estimated growth temperature of 4.2 ºC (Thiagarajan et al., 2011).[43] Guo et al. (2020) used model estimates to predict a negative correlation between Δ_{47} and Δ_{48} for cold-water corals, with kinetic effects causing enrichments in Δ_{47} and depletions in Δ_{48}, consistent with what we have observed for 47407 Coral.

Previous research has suggested that most biogenic and synthetic carbonates have a subtle offset from Δ_{47} equilibrium that is close to the detection limit.[16] In this study, our equilibrium regression based on theory and near-equilibrium calcites lies within the 95% confidence interval of our experimentally determined regression, however, a slight offset exists. The offset may exist because of subtle kinetic effects and/or vital effects present in carbonates that are used as standards.

3.6.c Comparison of Δ_{47} vs Δ_{48} equilibrium regressions using constant and regression AFFs

To further constrain the Δ_{47} vs Δ_{48} equilibrium relationship and quantify the effects of using a regression form AFF vs a constant AFF for $\Delta^*_{63\text{-}47}$ and $\Delta^*_{64\text{-}48}$, we have compared our Δ_{47} vs Δ_{48} equilibrium regressions in Equations 22 (derived from theory and a regression AFF) and 25 (derived from experimental data) to equilibrium regressions determined using constant AFFs.

Using the method described in Section 3.5, we determined the constant $\Delta^*_{63\text{-}47}$ and $\Delta^*_{64\text{-}48}$ values at 600 ºC to be 0.1881 and 0.1300, respectively. Equations 23 and 24 were used to calculate $\Delta_{47\ I\text{-}CDES\ EQ}$ and $\Delta_{48\ CDES\ 90\ EQ}$. This same method was used to calculate constant $\Delta^*_{63\text{-}47}$ and $\Delta^*_{64\text{-}48}$ values at 33.7 ºC, which were determined to be 0.1949 and 0.1308, respectively.

Bajnai et al. (2020) calculated Δ_{47} vs Δ_{48} equilibrium by determining constant $\Delta^*_{63\text{-}47}$ and $\Delta^*_{64\text{-}48}$ values at 600 ºC using similar methods to what is described here, with the additional step of adding a constant value to all $\Delta_{47\ CDES\ 90\ EQ}$ and $\Delta_{48\ CDES\ 90\ EQ}$ values. In short, they took the combined ETH-1/ETH-2 average $\Delta_{47\ CDES\ 90}$ and $\Delta_{48\ CDES\ 90}$ measured values and subtracted the

theoretical Δ_{63} and Δ_{64} values (Equations 9 and 10) from Hill et al. (2014) for 600 ºC to determine AFFs at 600 ºC. Then added the AFFs to theoretical Δ_{63} and Δ_{64} to calculate equilibrium Δ_{47} and Δ_{48}. The Δ_{47} and Δ_{48} values for 33.7 ºC determined in that calculation were compared to their experimentally determined $\Delta_{47\ CDES\ 90}$ and $\Delta_{48\ CDES\ 90}$ values for their Devils Hole vein calcite sample (known precipitation temperature of 33.7 ºC, see section 2.2.c), DH-2-8. They determined the offset between their measured and calculated Δ_{47} and Δ_{48} values at 33.7 ºC, and applied the offset as a constant to all Δ_{47} and Δ_{48} values for temperatures from 0-1000 ºC. The constants added to their equilibrium $\Delta_{47\ CDES\ 90}$ and $\Delta_{48\ CDES\ 90}$ values were 0.010 and -0.021, respectively.

The use of a constant AFF determined at a high temperature (ie. 600 ºC) may not extrapolate well to lower temperatures due to the compositional dependence of $\Delta^*_{63\text{-}47}$ and $\Delta^*_{64\text{-}48}$ on the Δ_{63} and Δ_{64} of the carbonate mineral.[41] This is supported by the comparison of $\Delta_{47\ I\text{-}CDES\ EQ}$ and $\Delta_{48\ CDES\ 90\ EQ}$ regressions calculated using low temperature (33.7 ºC), high temperature (600 ºC), and regression AFFs (Figure 10). The equilibrium regressions calculated using constant AFFs determined at 600 ºC have a $\Delta_{47\ I\text{-}CDES}$ offset of ~0.007 from the Devils Hole sample (DH-2 average) precipitated at 33.7 ºC (Figure 10a). The opposite is true at higher temperatures, with equilibrium regressions using a constant AFF determined at 33.7 ºC having a $\Delta_{47\ I\text{-}CDES}$ offset of ~0.007 from the ETH-1 and ETH-2 standards equilibrated at 600 ºC (Figure 10b). The equilibrium regression using a regression AFF is not offset from the low or high temperature $\Delta_{47\ I\text{-}CDES}$ values. All equilibrium regressions determined in this study are within the 95 % confidence interval of the experimentally determined regression (Figure 10, Regression A).

The range for Δ_{48} is compressed relative to Δ_{47}, and this contributes to smaller effects in Δ_{48} when extrapolating AFFs. The equilibrium regressions using low temperature and high temperature AFFs differ by ~0.0008 in the low and high temperature range.

The equilibrium regression from Bajnai et al. (2020) has a significant offset from the equilibrium regression determined here. In the 0-40 ºC range, the $\Delta_{47\ I\text{-}CDES\ 90\ EQ}$ and $\Delta_{48\ CDES\ 90\ EQ}$ offsets of 0.009 and 0.014, respectively, are equivalent to the measured difference in the Devils Hole calcite values from the two different labs. In the 100-600 ºC range, the offset is more pronounced, with a difference of 0.0159 and 0.0130 for $\Delta_{47\ CDES\ 90\ EQ}$ and $\Delta_{48\ CDES\ 90\ EQ}$, respectively. This is likely due to the extrapolation of their equilibrium line to high temperatures. Even though their calculation initially used a 600 ºC AFF, their Δ_{47} and Δ_{48} values were shifted with a constant to align with their Devils Hole $\Delta_{47\ CDES\ 90}$ and $\Delta_{48\ CDES\ 90}$, making it have a significant offset from their ETH-1 and ETH-2 values. Additional offset may arise from the Δ_{47} data from this study that are calculated using the I-CDES reference frame, as theirs uses the CDES 90 reference frame with differing anchor standard values. The Δ_{48} from both groups uses the CDES 90 reference frame but has slightly different standard anchor values (see Section 2.2.a).

4. CONCLUSIONS

Our lab developed the conceptual framework for utilizing paired Δ_{47} and Δ_{48} measurements to assess equilibrium and kinetic isotope effects[14], and building on this work and subsequent important contributions to this literature [20, 21, 19], we now have established paired Δ_{47} and Δ_{48} carbonate standard values, and are one of two labs using paired Δ_{47} and Δ_{48} measurements to study equilibrium and kinetic isotope effects in carbonates. This study, which contains 5581 Δ_{47} and 4212 Δ_{48} measurements of carbonate standards, demonstrates that for both Δ_{47} and Δ_{48}, carbonate standard-based standardization is a robust technique that provides reproducible data across multiple mass spectrometer configurations, using different acid digestion systems and acid digestion temperatures. We use a kernel density estimate-based approach that is statistically rigorous, minimizes the risk of unintentionally introducing human error or biases, and is fully transparent and reproducible. A power analysis of our data indicates how to approach analytical design for determining Δ_{48}, given different instrument conditions (ion beam intensity, acid digestion system, integration time, and mode of standardization). Our equilibrated gas-based $\Delta_{47\ CDES\ 90}$ determinations support the new nominal ETH-1, ETH-2, and ETH-3 anchor values from Bernasconi et al. (2021), and the use of the I-CDES reference frame. Our work also supports the accuracy of carbonate standard Δ_{47} values from Upadhyay et al. (in review). We provide novel estimates for Δ_{48} for a suite of standards and carbonates.

Following the framework from Hill et al. (2014) and Tripati et al. (2015), we have constructed a temperature-dependent Δ_{47} vs Δ_{48} equilibrium regression that has good agreement with experimental data for 20 carbonate standards. The regressions for equilibrium and experimental data are within error of each other, validating the robustness of the regressions. The equilibrium Δ_{47} vs Δ_{48} regression presented here can be used both for calculating temperatures and for quantifying kinetic fractionations. Theoretical and experimental slope corrections can be applied to samples with kinetic biases to produce usable clumped isotope data.[14, 41, 21] Specifically, this regression can now be used to calculate kinetic trajectories, fingerprint processes, and study rates and timescales.

Previous theoretical predictions from Guo et al. (2009) stated that there was a dependence of the acid digestion fractionation factors (AFFs), $\Delta^*_{63\text{-}47}$ and $\Delta^*_{64\text{-}48}$, on the calcite mineral Δ_{63} and Δ_{64}. To constrain this dependence experimentally, we calculated AFFs using constants at low and high temperature, and an AFF based on a regression. The Δ_{47} vs Δ_{48} equilibrium regression using a regression based AFF had the best agreement with our experimentally produced equilibrium regression, and did not have offsets when extrapolated, as was observed in equilibrium regressions relying on constant AFFs.

Data Accessibility Statement

All code and raw data used in analyses are available for review at https://github.com/Tripati-Lab/Lucarelli-et-al. Upon acceptance for publication, code and raw data will be permanently archived at Dryad, a static link provided in the manuscript, and this section updated.

Acknowledgements

We thank lab members past and present for their work running standards, efforts in data entry, and contributions to discussions. This work was funded by DOE BES grant DE-FG02-13ER16402. HMC was supported through a postdoctoral fellowship by the Institutional Research and Academic Career Development Awards (IRACDA) program at UCLA (Award # K12 GM106996).

References

1. Schauble, E. A., Ghosh, P. & Eiler, J. M. Preferential formation of 13C–18O bonds in carbonate minerals, estimated using first-principles lattice dynamics. *Geochimica et Cosmochimica Acta* **70**, 2510–2529 (2006). https://doi.org/10.1016/j.gca.2006.02.011
2. Ghosh, P. *et al.* 13C–18O bonds in carbonate minerals: A new kind of paleothermometer. *Geochimica et Cosmochimica Acta* **70**, 1439–1456 (2006). https://doi.org/10.1016/j.gca.2005.11.014
3. Urey, H. C. The thermodynamic properties of isotopic substances. *J. Chem. Soc.* 562 (1947) https://doi.org/10.1039/JR9470000562
4. Passey, B. H. & Henkes, G. A. Carbonate clumped isotope bond reordering and geospeedometry. *Earth and Planetary Science Letters* **351–352**, 223–236 (2012). https://doi.org/10.1016/j.epsl.2012.07.021
5. Tripati, A. K. *et al.* 13C–18O isotope signatures and 'clumped isotope' thermometry in foraminifera and coccoliths. *Geochimica et Cosmochimica Acta* **74**, 5697–5717 (2010). https://doi.org/10.1016/j.gca.2010.07.006
6. Henkes, G. A. *et al.* Temperature evolution and the oxygen isotope composition of Phanerozoic oceans from carbonate clumped isotope thermometry. *Earth and Planetary Science Letters* **490**, 40–50 (2018). https://doi.org/10.1016/j.epsl.2018.02.001
7. Huntington, K. W., Wernicke, B. P. & Eiler, J. M. Influence of climate change and uplift on Colorado Plateau paleotemperatures from carbonate clumped isotope thermometry. *Tectonics* **29**, 2009TC002449 (2010). https://doi.org/10.1029/2009TC002449
8. Lechler, A. R., Niemi, N. A., Hren, M. T. & Lohmann, K. C. Paleoelevation estimates for the northern and central proto-Basin and Range from carbonate clumped isotope thermometry: Δ_{47} PALEOALTIMETRY OF BASIN AND RANGE. *Tectonics* **32**, 295–316 (2013). https://doi.org/10.1002/tect.20016
9. Eagle, R. A. *et al.* Body temperatures of modern and extinct vertebrates from 13C-18O bond abundances in bioapatite. *Proceedings of the National Academy of Sciences* **107**, 10377–10382 (2010). https://doi.org/10.1073/pnas.0911115107
10. Daëron, M. *et al.* 13C18O clumping in speleothems: Observations from natural caves and precipitation experiments. *Geochimica et Cosmochimica Acta* **75**, 3303–3317 (2011). https://doi.org/10.1016/j.gca.2010.10.032

11. Kimball, J., Eagle, R. & Dunbar, R. Carbonate "clumped" isotope signatures in aragonitic scleractinian and calcitic gorgonian deep-sea corals. *Biogeosciences* **13**, 6487–6505 (2016). https://doi.org/10.5194/bg-13-6487-2016
12. Affek, H. P., Bar-Matthews, M., Ayalon, A., Matthews, A. & Eiler, J. M. Glacial/interglacial temperature variations in Soreq cave speleothems as recorded by 'clumped isotope' thermometry. *Geochimica et Cosmochimica Acta* **72**, 5351–5360 (2008). https://doi.org/10.1016/j.gca.2008.06.031
13. Saenger, C. *et al.* Carbonate clumped isotope variability in shallow water corals: Temperature dependence and growth-related vital effects. *Geochimica et Cosmochimica Acta* **99**, 224–242 (2012). https://doi.org/10.1016/j.gca.2012.09.035
14. Tripati, A. K. *et al.* Beyond temperature: Clumped isotope signatures in dissolved inorganic carbon species and the influence of solution chemistry on carbonate mineral composition. *Geochimica et Cosmochimica Acta* **166**, 344–371 (2015). https://doi.org/10.1016/j.gca.2015.06.021
15. Lloyd, M. K., Eiler, J. M. & Nabelek, P. I. Clumped isotope thermometry of calcite and dolomite in a contact metamorphic environment. *Geochimica et Cosmochimica Acta* **197**, 323–344 (2017). https://doi.org/10.1016/j.gca.2016.10.037
16. Daëron, M. *et al.* Most Earth-surface calcites precipitate out of isotopic equilibrium. *Nat Commun* **10**, 429 (2019). https://doi.org/10.1038/s41467-019-08336-5
17. Hill, P. S., Tripati, A. K. & Schauble, E. A. Theoretical constraints on the effects of pH, salinity, and temperature on clumped isotope signatures of dissolved inorganic carbon species and precipitating carbonate minerals. *Geochimica et Cosmochimica Acta* **125**, 610–652 (2014). https://doi.org/10.1016/j.gca.2013.06.018
18. Hill, P. S., Schauble, E. A. & Tripati, A. Theoretical constraints on the effects of added cations on clumped, oxygen, and carbon isotope signatures of dissolved inorganic carbon species and minerals. *Geochimica et Cosmochimica Acta* **269**, 496–539 (2020). https://doi.org/10.1016/j.gca.2019.10.016
19. Guo, W. Kinetic clumped isotope fractionation in the DIC-H2O-CO2 system: Patterns, controls, and implications. *Geochimica et Cosmochimica Acta* **268**, 230–257 (2020). https://doi.org/10.1016/j.gca.2019.07.055
20. Fiebig, J. *et al.* Combined high−precision Δ48 and Δ47 analysis of carbonates. *Chemical Geology* **522**, 186–191 (2019). https://doi.org/10.1016/j.chemgeo.2019.05.019
21. Bajnai, D. *et al.* Dual clumped isotope thermometry resolves kinetic biases in carbonate formation temperatures. *Nat Commun* **11**, 4005 (2020). https://doi.org/10.1038/s41467-020-17501-0
22. Eiler, J. M. & Schauble, E. 18O13C16O in Earth's atmosphere. *Geochimica et Cosmochimica Acta* **68**, 4767–4777 (2004). https://doi.org/10.1016/j.gca.2004.05.035

23. Eiler, J. M. "Clumped-isotope" geochemistry—The study of naturally-occurring, multiply-substituted isotopologues. *Earth and Planetary Science Letters* **262**, 309–327 (2007). https://doi.org/10.1016/j.epsl.2007.08.020
24. Upadhyay, D. *et al. Carbonate clumped isotope analysis (Δ47) of 21 carbonate standards determined via gas source isotope ratio mass spectrometry on four instrumental configurations using carbonate-based standardization and multi-year datasets*. http://eartharxiv.org/repository/view/1848/ (in review) https://doi.org/10.31223/X5VC80
25. Dennis, K. J., Affek, H. P., Passey, B. H., Schrag, D. P. & Eiler, J. M. Defining an absolute reference frame for 'clumped' isotope studies of CO2. *Geochimica et Cosmochimica Acta* **75**, 7117–7131 (2011). https://doi.org/10.1016/j.gca.2004.05.035
26. Petersen, S. V. *et al.* Effects of Improved ^{17}O Correction on Interlaboratory Agreement in Clumped Isotope Calibrations, Estimates of Mineral-Specific Offsets, and Temperature Dependence of Acid Digestion Fractionation. *Geochem. Geophys. Geosyst.* **20**, 3495–3519 (2019). https://doi.org/10.1029/2018GC008127
27. Bernasconi, S. M. *et al.* InterCarb: A Community Effort to Improve Interlaboratory Standardization of the Carbonate Clumped Isotope Thermometer Using Carbonate Standards. *Geochem Geophys Geosyst* **22**, (2021). http://doi.org/10.1029/2020GC009588
28. Winograd, I. J. *et al.* Continuous 500,000-Year Climate Record from Vein Calcite in Devils Hole, Nevada. *Science* **258**, 255–260 (1992).
29. Coplen, T. B. Calibration of the calcite–water oxygen-isotope geothermometer at Devils Hole, Nevada, a natural laboratory. *Geochimica et Cosmochimica Acta* **71**, 3948–3957 (2007).
30. Kluge, T., Affek, H. P., Dublyansky, Y. & Spötl, C. Devils Hole paleotemperatures and implications for oxygen isotope equilibrium fractionation. *Earth and Planetary Science Letters* **400**, 251–260 (2014).
31. Winograd, I. J. *et al.* Devils Hole, Nevada, δ^{18}O record extended to the mid-Holocene. *Quat. res.* **66**, 202–212 (2006). https://doi.org/10.1126/science.258.5080.255
32. Brand, W. A., Assonov, S. S. & Coplen, T. B. Correction for the 17O interference in δ(13C) measurements when analyzing CO2 with stable isotope mass spectrometry (IUPAC Technical Report). *Pure and Applied Chemistry* **82**, 1719–1733 (2010). https://doi.org/10.1351/PAC-REP-09-01-05
33. Daëron, M., Blamart, D., Peral, M. & Affek, H. P. Absolute isotopic abundance ratios and the accuracy of Δ47 measurements. *Chemical Geology* **442**, 83–96 (2016). https://doi.org/10.1016/j.chemgeo.2016.08.014
34. Wang, Z., Schauble, E. A. & Eiler, J. M. Equilibrium thermodynamics of multiply substituted isotopologues of molecular gases. *Geochimica et Cosmochimica Acta* **68**, 4779–4797 (2004). https://doi.org/10.1016/j.gca.2004.05.039
35. R Core Team. R: A language and environment for statistical computing. (2021). https://www.R-project.org/

36. Sheather, S. J. & Jones, M. C. A Reliable Data-Based Bandwidth Selection Method for Kernel Density Estimation. *Journal of the Royal Statistical Society: Series B (Methodological)* **53**, 683–690 (1991). https://doi.org/10.1111/j.2517-6161.1991.tb01857.x
37. Deng, H. & Wickham, H. Density estimation in R. (2011). https://vita.had.co.nz/papers/density-estimation.pdf
38. J Pinheiro, Bates, D., DebRoy, S., Sarkar, D. & R Core Team. nlme: Linear and nonlinear mixed effects models. (2021). https://CRAN.R-project.org/package=nlme
39. Lenth, R. V. emmeans: Estimated marginal means, aka least-squares means. (2021). https://CRAN.R-project.org/package=emmeans
40. Champely, S. pwr: Basic Functions for Power Analysis. R package version 1.3-0. (2020). https://CRAN.R-project.org/package=pwr
41. Guo, W., Mosenfelder, J. L., Goddard, W. A. & Eiler, J. M. Isotopic fractionations associated with phosphoric acid digestion of carbonate minerals: Insights from first-principles theoretical modeling and clumped isotope measurements. *Geochimica et Cosmochimica Acta* **73**, 7203–7225 (2009). https://doi.org/10.1016/j.gca.2009.05.071
42. Bernasconi, S. M. *et al.* Reducing Uncertainties in Carbonate Clumped Isotope Analysis Through Consistent Carbonate-Based Standardization. *Geochem. Geophys. Geosyst.* **19**, 2895–2914 (2018). https://doi.org/10.1029/2017GC007385
43. Thiagarajan, N., Adkins, J. & Eiler, J. Carbonate clumped isotope thermometry of deep-sea corals and implications for vital effects. *Geochimica et Cosmochimica Acta* **75**, 4416–4425 (2011). https://doi.org/10.1016/j.gca.2011.05.004

Figure Captions

Figure 1. Examples of relationships between δ^{47} and Δ_{47}, and δ^{48} and Δ_{48}, for different instrument configurations. **(A)** δ^{47} raw vs Δ_{47} raw on Config. 1a on 9/28/2015, (B) δ^{48} raw vs Δ_{48} raw for Config. 1a on 9/28/2015, **(C)** δ^{47} raw vs Δ_{47} raw on Config. 1b on 2/3/2018, Configuration 1b, **(D)** δ^{48} raw vs Δ_{48} raw for Config. 1b, **(E)** δ^{47} raw vs Δ_{47} raw on Config. 2, **(F)** δ^{48} raw vs Δ_{48} raw for Config. 2 on 2/3/2018, **(G)** δ^{47} raw vs Δ_{47} raw on Config. 3 on 4/12/2019, **(H)** δ^{48} raw vs Δ_{48} raw for Config. 3 on 4/12/2019. The grey color denotes that Δ_{48} from Config. 3 was not included in the long-term standard and carbonate values (see Sections 2.4 and 2.6.b for details). The slope is determined on a 10-day moving interval to account for instrument drift and applied to standards and samples as the slope correction. Config. 1a used 1000 °C and 25 °C equilibrated gases relative to the working gas composition, and Configs. 1b, 2, and 3 used ETH-1 and ETH-2 for the slope correction.

Figure 2. Example of the quality control process we use. **A)** histogram of the raw replicate pool (N = 389); **B)** Density plot with histogram of the raw replicate pool and first recommended exclusions (solid vertical lines); **C)** Density plot of the replicate pool following initial exclusions using the nearest minima method (N = 378). Potential cuts at 1σ (innermost pair of solid vertical lines in orange), 2σ (middle pair of solid vertical lines in red), and 3σ (outermost pair of solid vertical lines in purple) are shown; **D)** Histogram of the final replicate pool following a 3σ exclusion (N = 376). Final data are normally distributed (Shapiro-Wilk, W = 0.994, p-value = 0.16). Note that the x and y axis scales differ between plots.

Figure 3. Plot showing comparison between anchor standard ETH-1, ETH-2, and ETH-3 $\Delta_{47\ CDES\ 90}$ values determined on Config. 1a in this study and Bernasconi et al. (2021). Results validate the accuracy of mean values for these anchor standards from Bernasconi et al. (2021). These results also demonstrate the accuracy and precision of data from this instrument configuration. The range of $\Delta_{47\ I\text{-}CDES}$ values between labs in Bernasconi et al. (2021) for ETH-1, ETH-2, and ETH-3 are 0.05-0.06 ‰. The range of $\Delta_{47\ I\text{-}CDES}$ values in our lab between instrumental configurations are 0.00-0.01 ‰. Error bars indicate 1 standard error.

Figure 4. Plot showing comparison between $\Delta_{47\ CDES\ 90}$ and $\Delta_{48\ CDES\ 90}$ values from this study with values from Fiebig et al. (2019). All data was standardized with 1000 and 25 °C equilibrated gas-based standardization. Error bars indicate 1 standard error.

Figure 5. Comparison between $\Delta_{47\ I\text{-}CDES}$ values for working standards (standards treated as unknowns) determined in this study on three instrument configurations to mean value and individual lab values reported by Bernasconi et al. (2021). Values from our lab are calculated using carbonate-based standardization. Results validate the accuracy of mean values from Bernasconi et al. (2021). These results also demonstrate the accuracy and precision of data from our different instrumental configurations. The range of $\Delta_{47\ I\text{-}CDES}$ values between labs in Bernasconi et al. (2021) for the given standards are 0.05-0.10 ‰.

The range of $\Delta_{47\ \text{I-CDES}}$ values in our lab between instrumental configurations are 0.00-0.02 ‰. Error bars indicate 1 standard error.

Figure 6. $\Delta_{47\ \text{I-CDES}}$ and $\Delta_{48\ \text{CDES 90}}$ values of carbonate standards and Devils Hole carbonates determined in this study compared to $\Delta_{47\ \text{CDES 90}}$ and $\Delta_{48\ \text{CDES 90}}$ values from Bajnai et al. (2020). Values from our lab are calculated using carbonate-based standardization. Error bars indicate 1 standard error.

Figure 7. Constraints on acid digestion fractionation factors. **(A)** Regression for theoretical Δ_{63} vs acid digestion fractionation factor, $\Delta^*_{63\text{-}47}$. **(B)** Regression for theoretical Δ_{64} vs acid digestion fractionation factor, $\Delta^*_{64\text{-}48}$. **(C)** Regression for temperature (°C) vs acid digestion fractionation factor, $\Delta^*_{63\text{-}47}$, where r^2 = 0.9999. **(D)** Regression for temperature (°C) vs acid digestion fractionation factor, where r^2 = 0.9992. **(E)** Regression for acid digestion fractionation factors, $\Delta^*_{63\text{-}47}$ vs $\Delta^*_{64\text{-}48}$, where r^2 = 1. Numbers on regression indicate temperature in Celsius.

Figure 8. Relationships for use in determining unknown sample acid digestions fractionation factors, $\Delta^*_{63\text{-}47}$ and $\Delta^*_{64\text{-}48}$, and calcite mineral clumped isotope values, Δ_{63} and Δ_{64}. **A)** Regression for $\Delta_{47\ \text{I-CDES}}$ vs acid digestion fractionation factor, $\Delta^*_{63\text{-}47}$. **B)** Regression for $\Delta_{48\ \text{CDES 90}}$ vs acid digestion fractionation factor, $\Delta^*_{64\text{-}48}$. **C)** Regression for $\Delta_{47\ \text{I-CDES}}$ vs theoretical Δ_{63}, where r^2 = 1. **D)** Regression for $\Delta_{48\ \text{CDES 90}}$ vs theoretical Δ_{64}, where r^2 = 1. Numbers on regressions indicate temperature in Celsius.

Figure 9. Temperature-dependent equilibrium Δ_{47} vs Δ_{48} regressions. Regression A was calculated using theoretical calcite equilibrium Δ_{63} and Δ_{64} (Hill et al., 2014; Tripati et al., 2015) combined with experimental data to determine acid digestion fractionation factors. Regression B is a second order polynomial fit through all standards and samples, with the exception of 47407 Coral, which may express kinetic bias. See text for Methods, and Results and Discussion for details. The light blue shading indicates the 95% confidence interval of Regression B. Error bars indicate 1 standard error.

Figure 10. Temperature-dependent equilibrium Δ_{47} and Δ_{48} regressions calculated using different acid digestion fractionation factors. Experimental data is best represented by an equilibrium regression calculated with a regression-based acid digestion fractionation factor. For the temperature ranges **(A)** 0-40 °C and **(B)** 100-600 °C, Δ_{47} and Δ_{48} offsets exist between equilibrium regressions calculated using constant acid digestion fractionation factors calculated at 33.7 °C, 600 °C, and a regression-based acid digestion fractionation factor. All regressions from this study are within the 95% confidence interval (light blue shading) of the experimentally determined regression, Equilibrium Regression B. Error bars indicate 1 standard error. Numbers on regressions indicate temperature in Celsius.

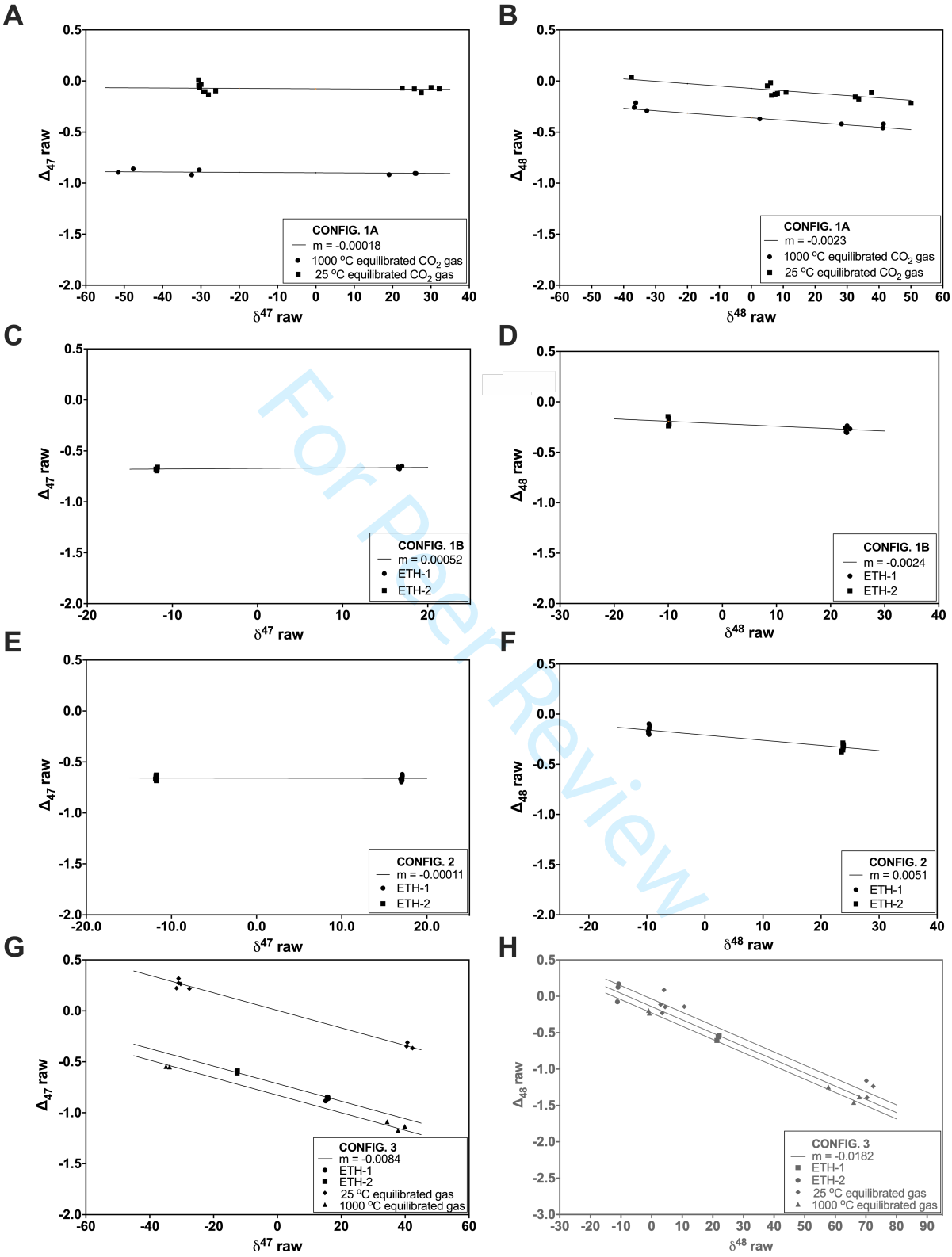

1074 Figure 1

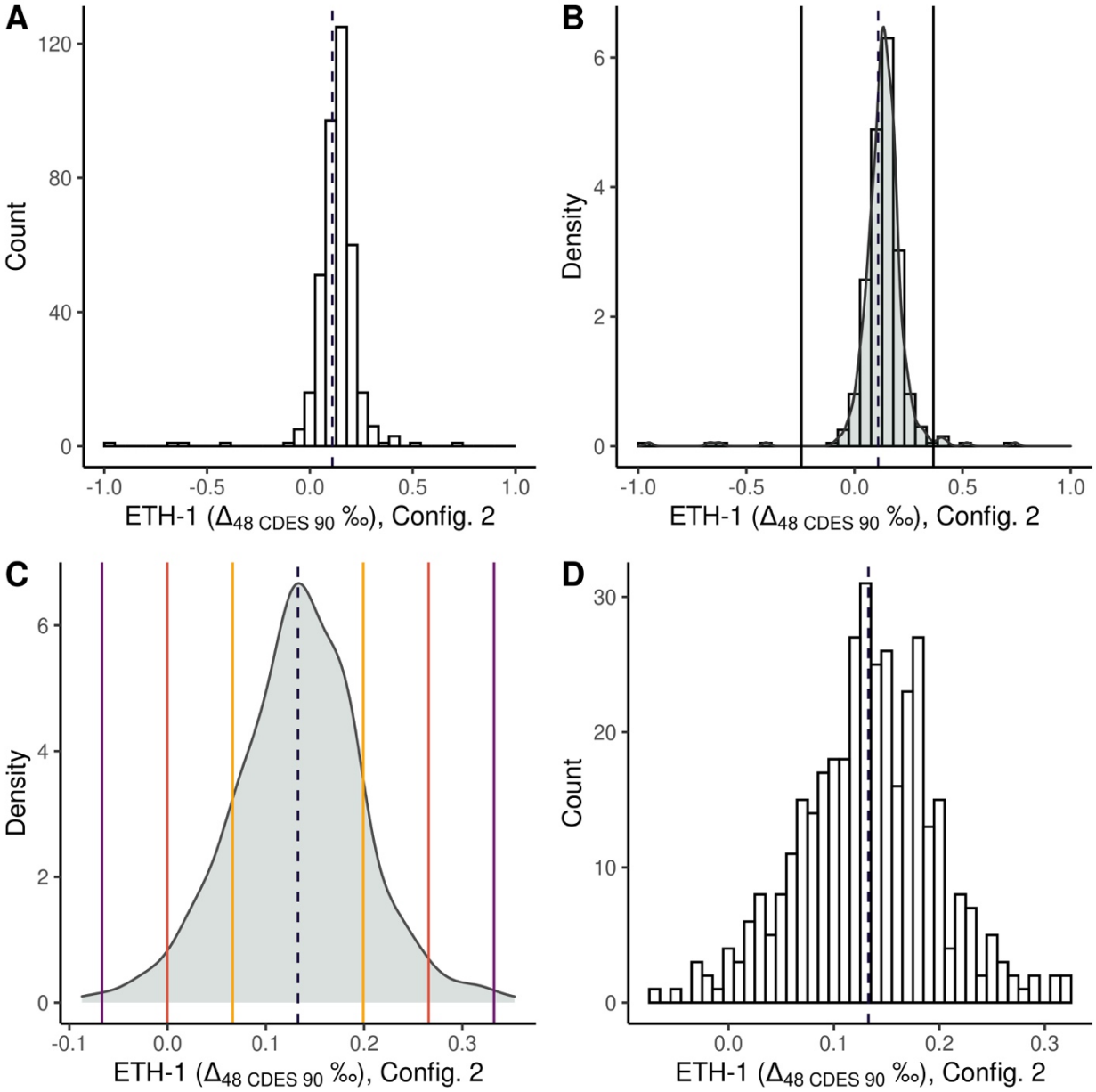
A
Count
ETH-1 (Δ48 CDES 90 ‰), Config. 2
B
Density
ETH-1 (Δ48 CDES 90 ‰), Config. 2
C
Density
ETH-1 (Δ48 CDES 90 ‰), Config. 2
D
Count
ETH-1 (Δ48 CDES 90 ‰), Config. 2

Figure 2

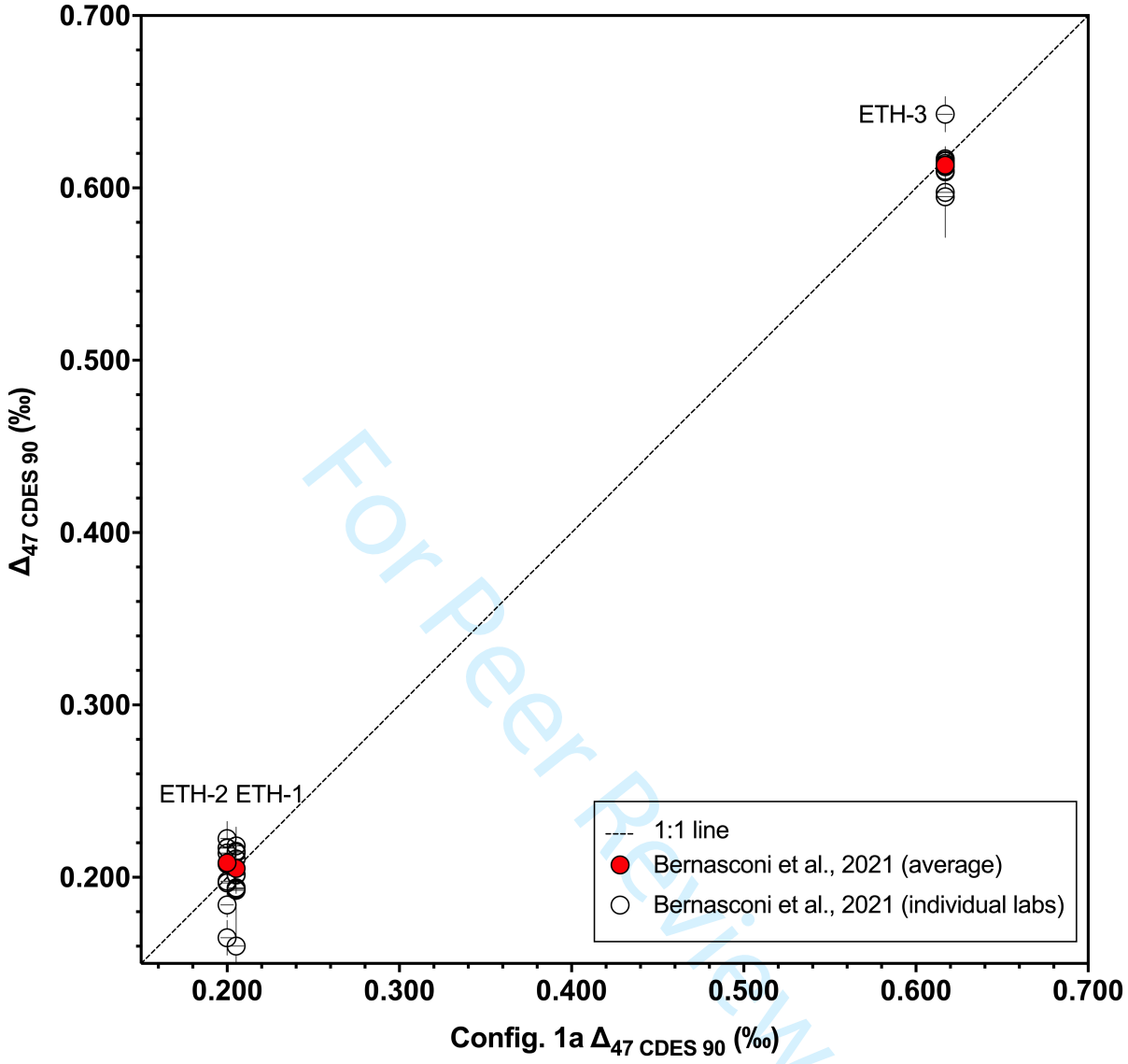

1077
1078 Figure 3

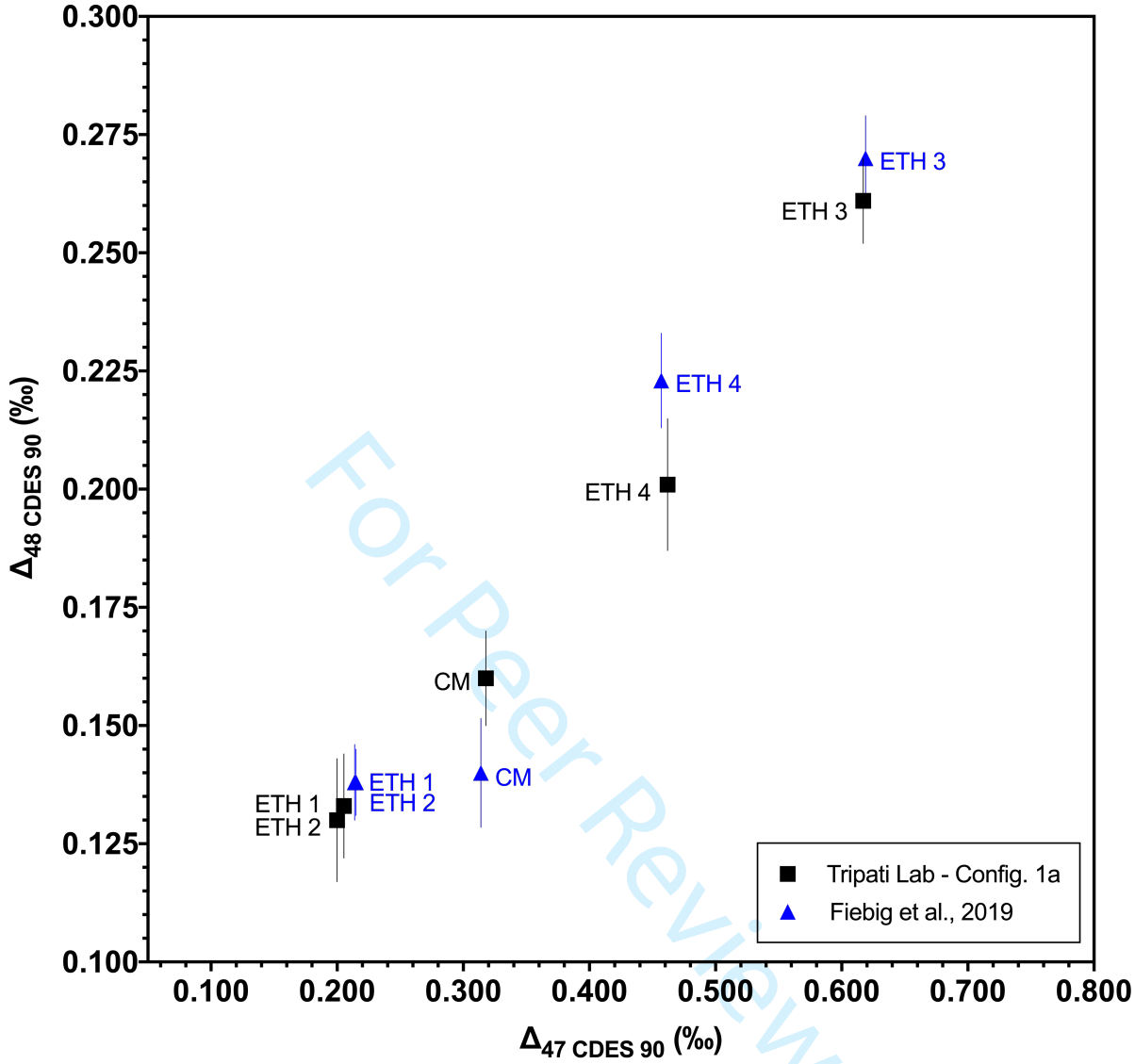

1079
1080 Figure 4

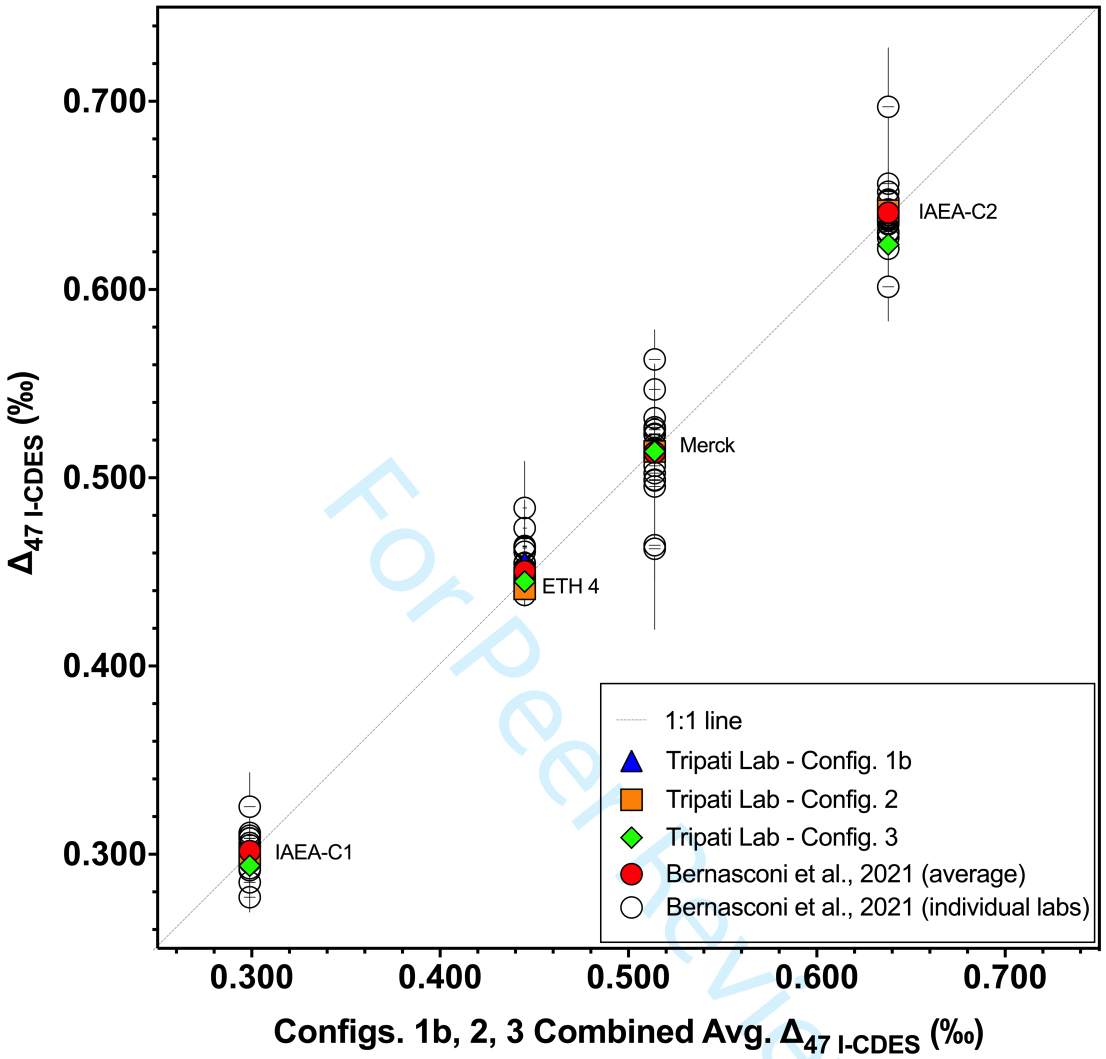

Figure 5

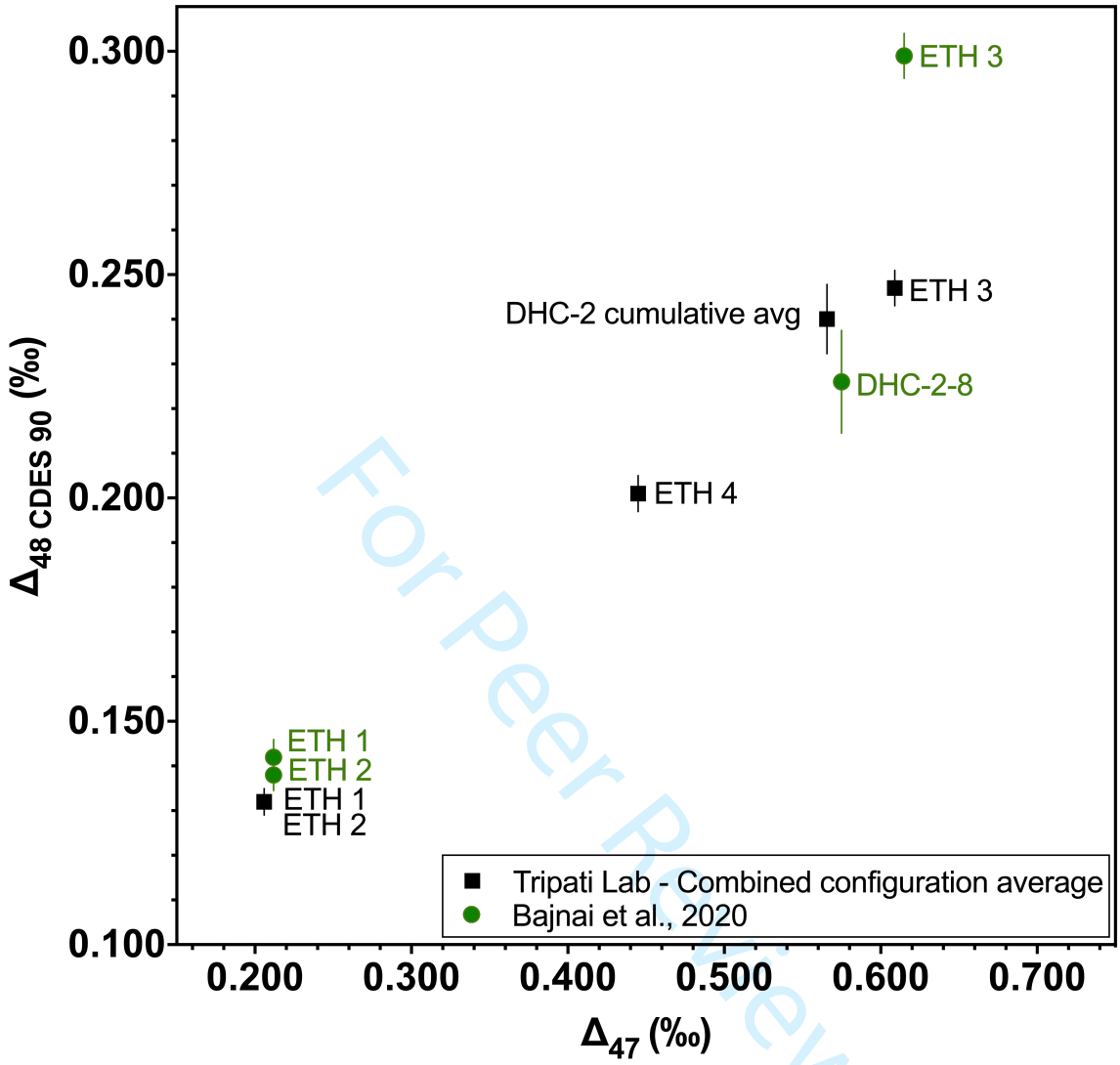

Figure 6

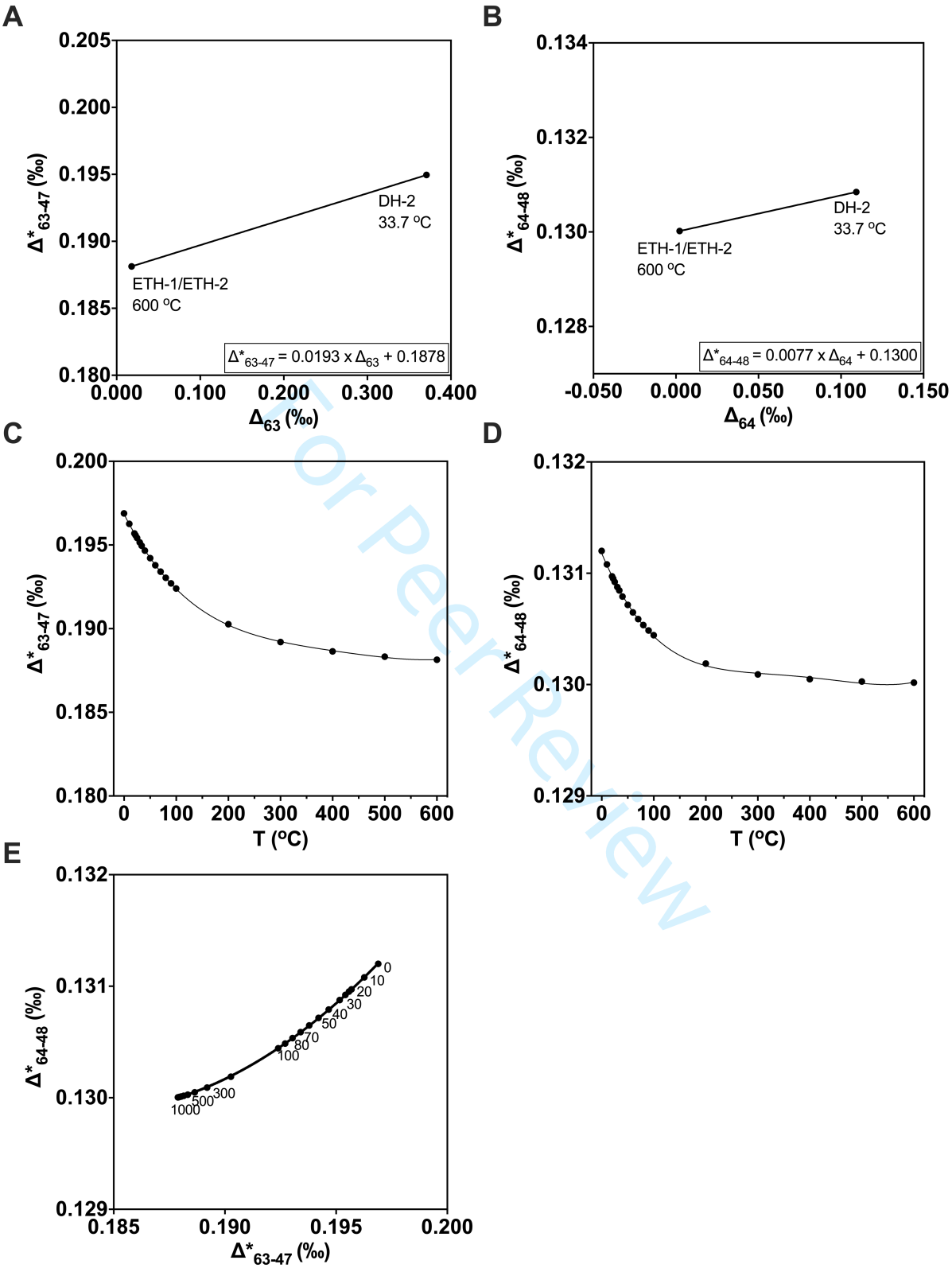

Figure 7

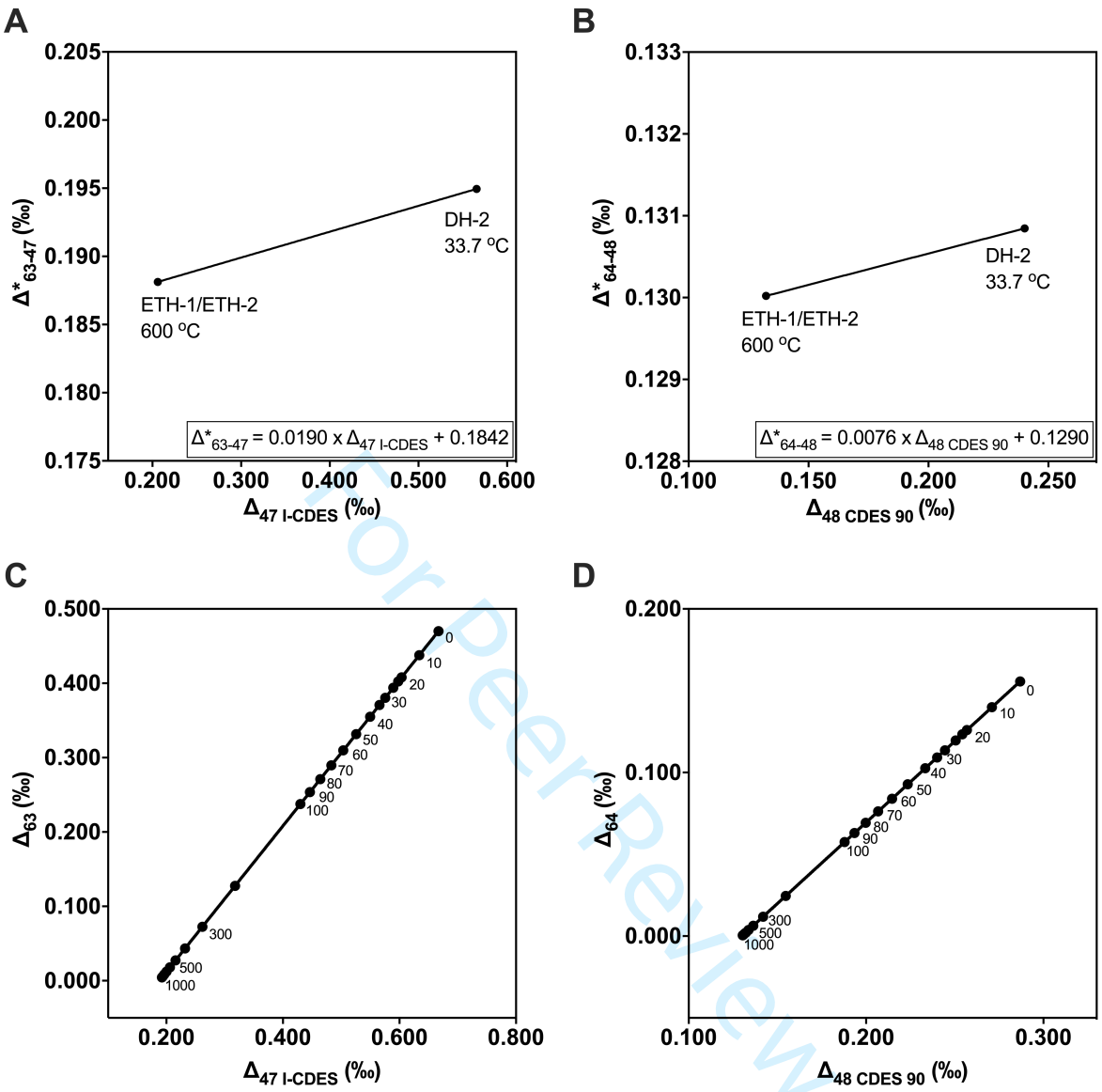

Figure 8

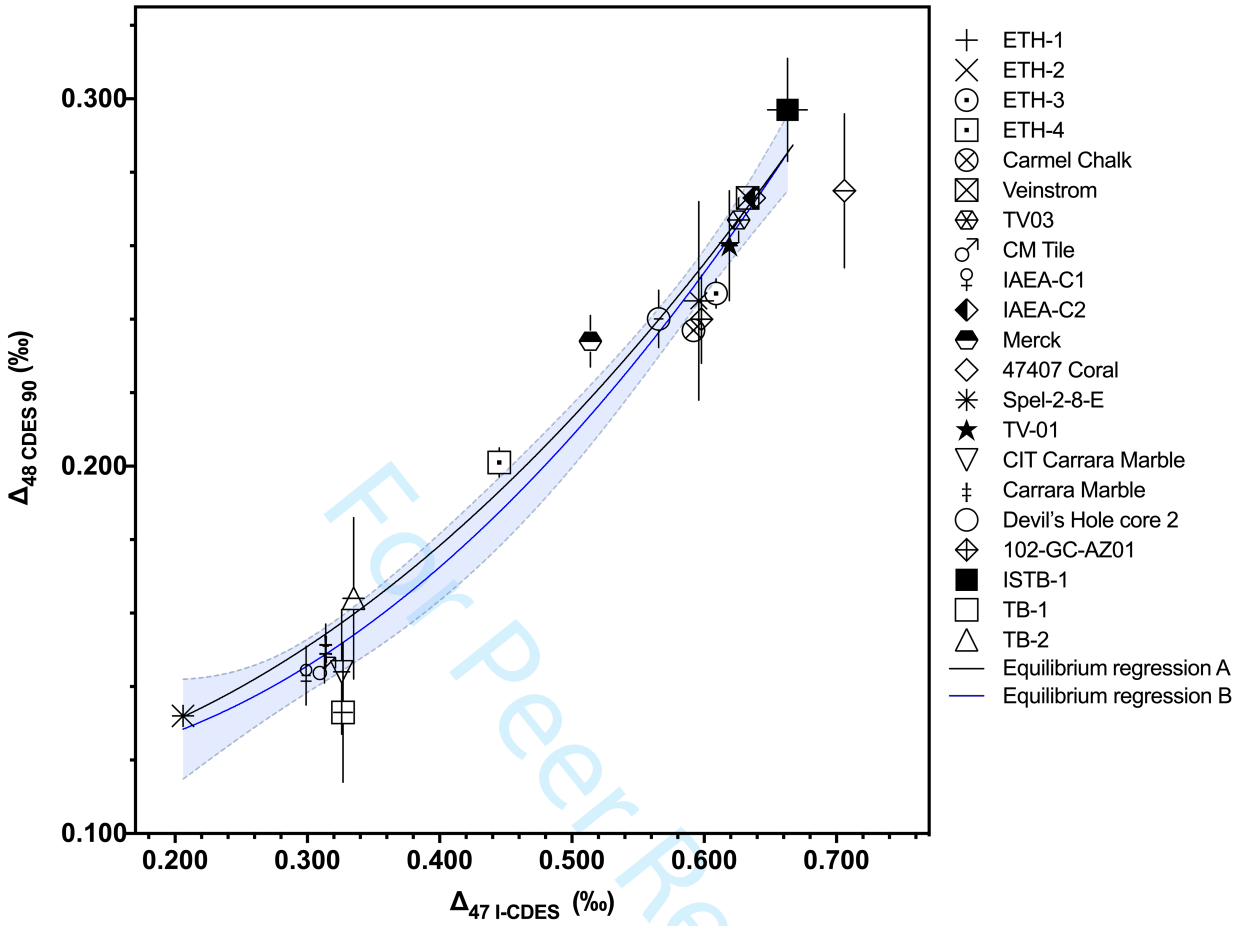

Figure 9

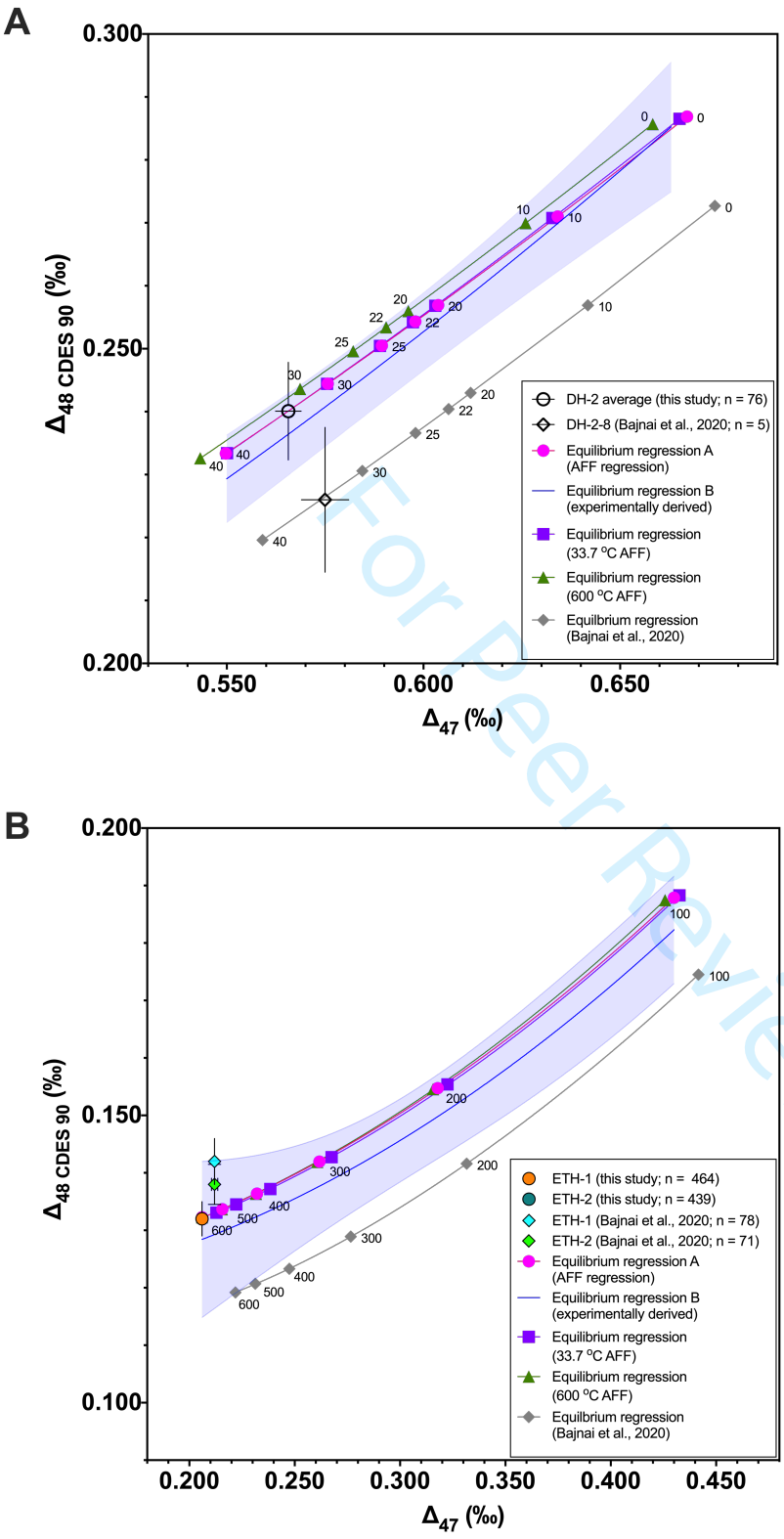

Figure 10

Standard	Mineralogy	Origin
102-GC-AZ01	calcite	Vein carbonate from Grand Canyon
Carmel Chalk	calcite	Chalk
Carrara Marble	calcite	Collected in Carrara, Tuscany, Italy.
CM Tile	calcite	Homogenized version of Carrara Marble (UCLA)
47407 Coral	Aragonite	Deep sea coral, *Desmophyllum*
DH-2-10	vein calcite	Devils Hole - U.S. Geological Survey, Ash Meadows, Nevada. Core 2. 172 ± 4 ka
DH-2-11	vein calcite	Devils Hole - U.S. Geological Survey, Ash Meadows, Nevada. Core 2. 163 ± 5 ka
DH-2-12	vein calcite	Devils Hole - U.S. Geological Survey, Ash Meadows, Nevada. Core 2. 157 ± 5 ka
DH-2-13	vein calcite	Devils Hole - U.S. Geological Survey, Ash Meadows, Nevada. Core 2. 151 ± 4 ka
ETH-1	calcite	Carrara Marble, heated to 600°C at 155 MPa for 10 hours, sent from ETH Zurich
ETH-2	calcite	Reagent grade synthetic, subjected to same treatment as ETH-1, sent from ETH Zurich
ETH-3	calcite	Upper Cretaceous chalk (mostly coccoliths), Isle of Rügen, Germany, sent from ETH Zurich
ETH-4	calcite	Same reagent grade synthetic as ETH-2, but unheated, sent from ETH Zurich
IAEA-C1	calcite	Carrara Marble, from International Atomic Energy Agency
IAEA-C2	travertine	Collected in Bavaria. From International Atomic Energy Agency
ISTB-1	Calcite	Speleothem from Yichang, Hubei province, China
Mallinckrodt	calcite	Synthetic, from Mallinckrodt Baker, Inc.
MERCK	calcite	Synthetic, from International Atomic Energy Agency
NBS 19	calcitic marble	Carrara Marble, from National Bureau of Standards
Spel 2-8-E	calcite	Speleothem
SRM 88B	dolomitic limestone	Collected from mine site near Skokie, Illinois, USA
TB-1	marble	Marble rock of marine origin from Quyang, Hebei province, China
TB-2	calcite	Hydrothermal calcite from Yanji, Jilin province, China
TV01	calcite	Travertine tile
TV03	calcite	Travertine tile
Veinstrom	vein calcite	Shallow carbonate vein collected from Tempiute Mountain, Nevada

Table 1. Description of the mineralogy and origin for 22 standards analyzed in this study (Upadhyay et al., 2021; Chang et al., 2020; Bernasconi et al., 2018) and 4 samples of Devils Hole carbonates. Uranium-series ages for Devil's Hole vein calcite were determined by Winograd et al., 2006.

Config.	Mass spectrometer model	Acid digestion temperature	Acid Digestion System, sample size	m/z 44 ion beam intensity	Integration time	Use of equilibrated gas- based corrections	Use of carbonate-based corrections	Δ_{47} reference frame	Δ_{48} reference frame
1a	Nu Instruments Perspective	90 °C	Common acid bath, 5-7 mg	80 nA before 6/2017, 60 nA after 6/2017	1600 s	Yes, 25 and 1000 °C equilibrated gases	No	CDES 90	CDES 90
1b	Nu Instruments Perspective	90 °C	Common acid bath, 5-7 mg	80 nA before 6/2017, 60 nA after 6/2017	1600 s	No	Yes	I-CDES	CDES 90
1c	Nu Instruments Perspective	90 °C	Common acid bath, 0.45-0.60 mg	80-30 nA	1200 s	No	Yes	I-CDES	CDES 90
2	Nu Instruments Perspective	70 °C	Nu Carb, 0.45-0.60 mg	80-30 nA	1200 s	No	Yes	I-CDES	CDES 90
3	Thermo Finnigan MAT 253	90 °C	Common acid bath 5-7 mg	16 V	720 s	No	Yes	I-CDES	N/A

Table 2. Description of mass spectrometer configurations used in this study.

Standard	$\Delta_{47\ CDES\ 90}$ (‰) This work	N	Δ_{47} SD	Δ_{47} SE	$\Delta_{47\ CDES\ 90}$ (‰) Bernasconi et al., 2021	N	Δ_{47} SD	Δ_{47} SE	Difference in $\Delta_{47\ CDES\ 90}$ (‰)
Carmel Chalk	0.607	46	0.012	0.002					
Carrara Marble	0.318	62	0.030	0.004					
ETH-1	0.205	36	0.026	0.004	0.205	232	0.024	0.002	0.000
ETH-2	0.200	30	0.023	0.004	0.208	215	0.022	0.001	-0.008
ETH-3	0.617	35	0.017	0.003	0.613	264	0.023	0.001	0.004
ETH-4	0.462	36	0.026	0.004	0.450	162	0.023	0.002	0.012
TV03	0.637	56	0.036	0.005					
Veinstrom	0.643	69	0.032	0.004					

Table 3. $\Delta_{47\ CDES\ 90}$ relative to 25 and 1000 °C equilibrated gases analyzed on Config. 1a from this study and $\Delta_{47\ CDES\ 90}$ values from Bernasconi et al., 2021. The values shaded in gray were used as anchors for carbonate standard based standardization in this study.

Standard	$\Delta_{48\ CDES\ 90}$ (‰)	N	Δ_{48} SD	Δ_{48} SE	Fiebig et al., 2019 $\Delta_{48\ CDES\ 90}$ (‰)	N	Δ_{48} SE	Difference in $\Delta_{48\ CDES\ 90}$ (‰)
Carmel Chalk	0.261	71	0.058	0.007				
Carrara Marble	0.160	64	0.081	0.010	0.140	12	0.011	0.020
ETH-1	0.133	44	0.076	0.011	0.138	19	0.008	-0.005
ETH-2	0.130	36	0.082	0.013	0.138	18	0.007	-0.008
ETH-3	0.261	45	0.059	0.009	0.270	16	0.009	-0.009
ETH-4	0.201	45	0.093	0.014	0.223	11	0.010	-0.022
TV03	0.269	55	0.054	0.007				
Veinstrom	0.263	74	0.083	0.010				

Table 4. $\Delta_{48\ CDES\ 90}$ for carbonate standards analyzed on Config. 1a. All data in this table was standardized using only 25 and 1000 ºC equilibrated gases for linearity corrections and transfer functions. Results are compared to values from Fiebig et al., 2019.

Standard	Config. 1b				Config. 2				Config. 3			
	Δ_{47} I-CDES (‰)	N	Δ_{47} SD	Δ_{47} SE	Δ_{47} I-CDES (‰)	N	Δ_{47} SD	Δ_{47} SE	Δ_{47} I-CDES (‰)	N	Δ_{47} SD	Δ_{47} SE
Carmel Chalk	0.591	94	0.017	0.002	0.589	248	0.026	0.002	0.594	282	0.021	0.001
Carrara Marble	0.312	81	0.031	0.003	0.328	44	0.048	0.007	0.310	155	0.020	0.002
CMTile					0.315	303	0.029	0.002	0.310	160	0.019	0.001
ETH-1	0.205	81	0.021	0.002	0.205	402	0.026	0.001	0.206	284	0.020	0.001
ETH-2	0.208	69	0.020	0.002	0.206	386	0.027	0.001	0.207	271	0.024	0.001
ETH-3	0.612	69	0.023	0.003	0.602	184	0.027	0.002	0.614	210	0.022	0.002
ETH-4	0.455	64	0.020	0.003	0.441	191	0.026	0.002	0.445	2087	0.021	0.001
IAEA-C1					0.300	68	0.025	0.003	0.294	15	0.017	0.004
IAEA-C2					0.642	60	0.025	0.003	0.624	14	0.021	0.005
Mallinckrodt									0.465	16	0.042	0.011
Merck					0.514	67	0.03	0.004	0.514	14	0.030	0.008
NBS 19									0.316	8	0.025	0.009
SRM88B									0.528	11	0.017	0.005
TV03	0.626	47	0.019	0.003					0.626	80	0.019	0.002
Veinstrom	0.636	102	0.026	0.003	0.634	322	0.030	0.002	0.632	304	0.023	0.001

Table 5. $\Delta_{47\ \text{I-CDES}}$ data for Config. 1b, 2, and 3. All data in this table used carbonate-based standardization. The standards used as anchors for standardization in each configuration are shaded gray, with all other standards treated as unknowns.

Standard	Config. 1b, 2, 3 combined average				Upadhyay et al., in review				Diff.	Bernasconi et al., 2021 average				Diff.
	Δ_{47} I-CDES (‰)	N	Δ_{47} SD	Δ_{47} SE	Δ_{47} I-CDES (‰)	N	Δ_{47} SD	Δ_{47} SE		Δ_{47} I-CDES (‰)	N	Δ_{47} SD	Δ_{47} SE	
102-GC-AZ01	0.598	24	0.028	0.006	0.608	15	0.023	0.006	-0.010					
Carmel Chalk	0.592	640	0.025	0.001	0.591	90	0.019	0.002	0.001					
Carrara Marble	0.314	280	0.030	0.002	0.311	81	0.027	0.003	0.003					
Carrara Marble CIT	0.326	21	0.027	0.006	0.325	4	0.008	0.004	0.001					
CMTile	0.313	463	0.026	0.001	0.308	13	0.022	0.006	0.005					
47407 Coral	0.707	9	0.025	0.008	0.664	6	0.012	0.005	0.043					
DH-2-10	0.554	11	0.013	0.004										
DH-2-11	0.560	19	0.027	0.006										
DH-2-12	0.564	18	0.025	0.006										
DH-2-13	0.568	17	0.027	0.006										
DH-2 Combined	0.566	74	0.028	0.003										
ETH-1	0.206	767	0.023	0.001	0.212	59	0.023	0.003	-0.006					
ETH-2	0.206	726	0.025	0.001	0.218	90	0.019	0.002	-0.012					
ETH-3	0.609	463	0.025	0.001	0.617	49	0.021	0.003	-0.008					
ETH-4	0.445	463	0.023	0.001	0.457	72	0.0017	0.002	-0.012	0.4511	945	0.0338	0.0011	-0.006
IAEA-C1	0.299	83	0.024	0.003	0.305	25	0.025	0.005	-0.006	0.3018	310	0.0229	0.0013	-0.003
IAEA-C2	0.638	74	0.025	0.003	0.643	21	0.023	0.005	-0.005	0.6409	333	0.0292	0.0016	-0.003
ISTB-1	0.663	15	0.059	0.015	0.609	10	0.041	0.013	0.054					
Mallinckrodt	0.465	16	0.042	0.011	0.468	13	0.039	0.011	-0.003					
Merck	0.514	81	0.030	0.003	0.526	22	0.028	0.006	-0.012	0.5135	286	0.0406	0.0024	<0.001
NBS 19	0.316	8	0.025	0.009	0.319	7	0.024	0.009	-0.003					
SPEL-2-8-E	0.596	11	0.035	0.011	0.593	10	0.038	0.012	0.003					
SRM88B	0.528	11	0.017	0.005	0.503	12	0.007	0.002	0.025					
TB-1	0.327	21	0.034	0.007	0.313	5	0.009	0.004	0.014					
TB-2	0.335	19	0.035	0.008	0.326	2	0.036	0.026	0.009					
TV01	0.619	22	0.028	0.006	0.645	3	0.011	0.006	-0.026					
TV03	0.626	127	0.019	0.002	0.622	44	0.020	0.003	0.004					
Veinstrom	0.633	728	0.026	0.001	0.637	90	0.019	0.002	-0.004					

Table 6. Config. 1b, 2, 3 combined average $\Delta_{47\ \text{I-CDES}}$ for all standards, with comparison to $\Delta_{47\ \text{I-CDES}}$ from Upadhyay et al. (in review), and $\Delta_{47\ \text{I-CDES}}$ for working standards (standards treated as unknowns) from Bernasconi et al. (2021). $\Delta_{47\ \text{I-CDES}}$ from Upadhyay et al. (in review) were calculated using the transfer function $^{\text{new}}\Delta_{47} = 0.048529 - 0.000165 \times \delta_{47} + 0.944081 \times {}^{\text{old}}\Delta_{47}$ (Bernasconi et al., 2021), where $^{\text{old}}\Delta_{47}$ are Δ_{47} values determined using previously published values for ETH anchor standards from Bernasconi et al. (2018).

Standard	Config. 1b				Config. 2				*Config. 3*				Config. 1b, 2 Combined Average			
	Δ_{48} CDES 90 (‰)	N	Δ_{48} SD	Δ_{48} SE	Δ_{48} CDES 90 (‰)	N	Δ_{48} SD	Δ_{48} SE	*Δ_{48} CDES 90 (‰)*	*N*	*Δ_{48} SD*	*Δ_{48} SE*	Δ_{48} CDES 90 (‰)	N	Δ_{48} SD	Δ_{48} SE
102-GC-AZ01													0.240	24	0.057	0.012
Carmel Chalk	0.243	69	0.028	0.003	0.235	250	0.062	0.004	*0.227*	*166*	*0.080*	*0.006*	0.237	319	0.056	0.003
Carrara Marble	0.146	81	0.072	0.008	0.159	54	0.065	0.009	*0.175*	*80*	*0.161*	*0.018*	0.151	135	0.079	0.006
Carrara Marble CIT													0.144	24	0.081	0.017
CMTile	0.149	18	0.029	0.007	0.145	291	0.060	0.004	*0.156*	*144*	*0.098*	*0.008*	0.145	309	0.059	0.003
47407 Coral													0.275	11	0.071	0.021
DH-2-10													0.236	16	0.082	0.020
DH-2-11													0.196	17	0.035	0.009
DH-2-12													0.243	16	0.032	0.008
DH-2-13													0.261	19	0.063	0.014
DH-2 Combined													0.240	76	0.068	0.008
ETH-1	0.130	88	0.051	0.005	0.133	376	0.065	0.003	*0.139*	*188*	*0.105*	*0.008*	0.132	464	0.062	0.003
ETH-2	0.131	73	0.064	0.008	0.133	366	0.056	0.003	*0.156*	*204*	*0.110*	*0.008*	0.132	439	0.058	0.003
ETH-3	0.244	68	0.054	0.007	0.249	168	0.058	0.004	*0.250*	*145*	*0.082*	*0.007*	0.247	236	0.057	0.004
ETH-4	0.198	70	0.059	0.007	0.203	187	0.058	0.004	*0.206*	*171*	*0.106*	*0.008*	0.201	257	0.058	0.004
IAEA-C1					0.143	49	0.056	0.008	*0.142*	*15*	*0.141*	*0.036*	0.143	49	0.056	0.008
IAEA-C2					0.273	59	0.062	0.008	*0.236*	*13*	*0.067*	*0.018*	0.273	59	0.062	0.008
ISTB-1													0.297	12	0.047	0.014
Mallinckrodt									*0.136*	*13*	*0.081*	*0.023*				
MERCK					0.234	59	0.055	0.007	*0.175*	*11*	*0.170*	*0.051*	0.234	59	0.055	0.007
NBS-19									*0.116*	*7*	*0.073*	*0.027*				
SRM 88B									*0.424*	*10*	*0.153*	*0.048*				
SPEL-2-8-E													0.245	11	0.089	0.027
TB-1													0.133	23	0.089	0.019
TB-2													0.164	19	0.095	0.022
TV01													0.260	25	0.077	0.015
TV03	0.267	58	0.043	0.006					*0.212*	*32*	*0.063*	*0.011*	0.267	58	0.043	0.006
Veinstrom	0.272	100	0.066	0.007	0.274	336	0.059	0.003	*0.252*	*193*	*0.079*	*0.006*	0.273	436	0.061	0.003

Table 7. $\Delta_{48\ \mathrm{CDES\ 90}}$ data for the Config. 1b, 2, and 3. All $\Delta_{48\ \mathrm{CDES\ 90}}$ data in this table used carbonate-based standardization. Config. 3 (gray text) data was not included in the combined instrument average (see Results and Discussion for details). The standards used for standardization in each configuration are shaded gray, with all other standards being treated as unknowns.

Sample	Cumulative avgs.				Bajnai et al. (2020)					Cumulative avgs.				Bajnai et al. (2020)				
	$\Delta_{47\ I\text{-}CDES}$ (‰)	N	Δ_{47} SD	Δ_{48} SE	$\Delta_{47\ CDES\ 90}$ (‰)	N	Δ_{47} SD	Δ_{47} SE	Diff.	$\Delta_{48\ CDES\ 90}$ (‰)	N	Δ_{48} SD	Δ_{48} SE	$\Delta_{48\ CDES\ 90}$ (‰)	N	Δ_{48} SD	Δ_{48} SE	Diff.
DH-2-10	0.554	11	0.013	0.004						0.236	16	0.082	0.020					
DH-2-11	0.560	19	0.027	0.006						0.196	17	0.035	0.009					
DH-2-12	0.564	18	0.025	0.006						0.243	16	0.032	0.008					
DH-2-13	0.568	17	0.027	0.006						0.261	19	0.063	0.014					
DH-2 Avg	**0.566**	**74**	**0.028**	**0.003**						**0.240**	**76**	**0.068**	**0.008**					
DH-2-8					**0.575**	**5**	**0.007**	**0.003**						**0.226**	**5**	**0.026**	**0.012**	
ETH-1	0.206	767	0.023	0.001	0.212	78	0.010	0.001	-0.006	0.132	464	0.062	0.003	0.142	78	0.036	0.004	-0.010
ETH-2	0.206	726	0.025	0.001	0.212	71	0.011	0.001	-0.006	0.132	439	0.058	0.003	0.138	71	0.029	0.003	-0.006
ETH-3	0.609	463	0.025	0.001	0.615	74	0.010	0.001	-0.006	0.247	236	0.057	0.004	0.299	74	0.042	0.010	-0.052

Table 8. Long-term $\Delta_{47\ I\text{-}CDES}$, $\Delta_{47\ CDES\ 90}$, and $\Delta_{48\ CDES\ 90}$ values from this study and Bajnai et al. (2020) using carbonate standard-based standardization. Bolded samples are Devils Hole vein calcite from Cave 2 (DH-2), from sites 10, 11, 12, 13, and 8. DH-2 Avg is the Cave 2 average from this study of sections 10, 11, 12, and 13.

Temperature	Δ_{63} (Hill et al., 2014; Tripati et al., 2015)	$\Delta^*_{63\text{-}47}$	$\Delta_{47\ \text{I-CDES EQ}}$	Δ_{64} (Hill et al., 2014; Tripati et al., 2015)	$\Delta^*_{64\text{-}48}$	$\Delta_{48\ \text{CDES 90 EQ}}$
0	0.4701	0.1969	0.6670	0.1557	0.1312	0.2869
10	0.4378	0.1963	0.6341	0.1399	0.1311	0.2710
20	0.4080	0.1957	0.6037	0.1260	0.1310	0.2569
22	0.4024	0.1956	0.5979	0.1234	0.1310	0.2543
25	0.3940	0.1954	0.5894	0.1196	0.1309	0.2505
30	0.3805	0.1952	0.5757	0.1136	0.1309	0.2445
33.7 (DH-2)	0.3707	0.1949	0.5657	0.1092	0.1308	0.2401
40	0.3551	0.1947	0.5498	0.1026	0.1308	0.2334
50	0.3316	0.1942	0.5258	0.0928	0.1307	0.2235
60	0.3098	0.1938	0.5036	0.0840	0.1306	0.2147
70	0.2897	0.1934	0.4831	0.0762	0.1306	0.2068
80	0.2710	0.1930	0.4641	0.0693	0.1305	0.1998
90	0.2537	0.1927	0.4464	0.0630	0.1305	0.1935
100	0.2376	0.1924	0.4300	0.0575	0.1304	0.1879
200	0.1276	0.1903	0.3179	0.0246	0.1302	0.1547
300	0.0726	0.1892	0.2618	0.0119	0.1301	0.1420
400	0.0435	0.1886	0.2321	0.0063	0.1300	0.1364
500	0.0273	0.1883	0.2157	0.0037	0.1300	0.1337
600	0.0179	0.1881	0.2061	0.0022	0.1300	0.1323
700	0.0122	0.1880	0.2002	0.0015	0.1300	0.1315
800	0.0085	0.1880	0.1965	0.0010	0.1300	0.1310
900	0.0061	0.1879	0.1940	0.0007	0.1300	0.1307
1000	0.0045	0.1879	0.1924	0.0005	0.1300	0.1305

Table 9. Theoretical model equilibrium Δ_{63} and Δ_{64} for calcite (Hill et al., 2014; Tripati et al., 2015), acid digestion fractionation factors $\Delta^*_{63\text{-}47}$ and $\Delta^*_{64\text{-}48}$ for the phosphoric acid digestion of calcite to CO_2, and equilibrium calcite $\Delta_{47\ \text{I-CDES EQ}}$ and $\Delta_{48\ \text{CDES 90 EQ}}$.